„Dunărea de Jos" University of Galaţi
Fundamental and Engineering Science Doctoral School

# DOCTOR OF PHILOSOPHY DEGREE

# PhD THESIS

## SUMMARY

# Functional surfaces obtained by electrochemical methods and their characterization

**PhD student,**
**ec. Valentin Marian DUMITRAȘCU**

**Supervisor,**
**Prof. univ. dr. chim. Lidia BENEA**

**Series I 5: Materials Engineering Nr. 11**
**GALAŢI**
**2018**

**„Dunărea de Jos" University of Galaţi**

**Fundamental and Engineering Science Doctoral School**

# DOCTOR OF PHILOSOPHY DEGREE

# PhD THESIS

## SUMMARY

# Functional surfaces obtained by electrochemical methods and their characterization

**PhD student,**

**ec. Valentin Marian DUMITRAȘCU**

| | |
|---|---|
| **President** | Prof. univ. dr. eng. Iulian Gabriel BÎRSAN |
| **Supervisor** | Prof. univ. dr. chim. Lidia BENEA |
| **Scientific References** | Prof. univ. dr. eng. Leandru Gheorghe BUJOREANU |
| | Prof. univ. dr. eng. Cristian PREDESCU |
| | Prof. univ. dr. phys. Adrian CÎRCIUMARU |

**Series I 5: Materials Engineering Nr. 11**

**GALAȚI**

**2018**

Seriile tezelor de doctorat sustinute public în UDJG începând cu 1 octombrie 2013 sunt:

Domeniul **ȘTIINȚE INGINEREȘTI**

- Seria I 1: **Biotehnologii**
- Seria I 2: **Calculatoare și tehnologia informației**
- Seria I 3. **Inginerie electrică**
- Seria I 4: **Inginerie industrială**
- Seria I 5: **Ingineria materialelor**
- Seria I 6: **Inginerie mecanică**
- Seria I 7: **Ingineria produselor alimentare**
- Seria I 8: **Ingineria sistemelor**

Domeniul **ȘTIINȚE ECONOMICE**

- Seria E 1: **Economie**
- Seria E 2: **Management**

Domeniul **ȘTIINȚE UMANISTE**

- Seria U 1: **Filologie- Engleză**
- Seria U 2: **Filologie- Română**
- Seria U 3: **Istorie**

The science of today
is the technology of tomorrow.

Edward Teller

# ACKNOWLEDGEMENTS

The PHD thesis was elaborated in Competences Center Interface-Tribocorrosion and Electrochemical Systems (CC-ITES) from „Dunărea de Jos" University of Galați coordinated by prof.univ.dr. chim. Lidia Benea.

I want to start expressing sincere acknowledgements to my supervisor prof. univ. dr. chim. Lidia Benea who guided me with patience in the scientific research mysteries, for support, advices and encouragement offered to finish this phase of my academic path.

In addition, i would like to thank once more prof. univ. dr. chim. Lidia BENEA for including me in the work group of the research project UEFISCDI – PNII-PCE – 10(2013 – 2016) HyBioElect – „New hybrid (inorganic-organic) functionalization of biomaterials (metals alloys) surfaces with functional molecules by electrochemical techniques" that helped me to develop the research competences and achieve experience in the electrochemistry domain, and also, for the financial support that granted various participations to international conferences in order to achieve the research objectives.

I express sincere acknowledgments to the official references: Mr. prof. univ. dr. eng. Leandru Gheorghe Bujoreanu, Mr. prof. univ. dr. eng. Cristian Predescu, Mr. prof. univ. dr. phys. Adrian Cîrciumaru, for the honor of examining my PHD thesis and for the evaluation reports. I also wish to thank Prof. dr. ing. eng. Iulian Gabriel Bîrsan for the honor of accepting the president position of the evaluation commission.

I would like to give special thanks for the guidance commision formed by Ș.L. dr. chim. Alina Mureșan, Conf. univ. dr. eng. Ștefan Baltă, pro-rector of "Dunărea de Jos„ University of Galați and Prof. univ. dr. eng. Marian Bordei, dean of Engineering Faculty of „Dunărea de Jos" University of Galați

It is due to express special thanks to Prof. univ. dr. eng. Iulian Gabriel Bîrsan, Prof. dr. phys. Adrian Cîrciumaru and Ș.L. dr. eng. Iulia Graur for their patience and guidance during the friction tests and for providing me access in the laboratory of Research and Development Center for Thermoset Composites Center of „Dunărea de Jos" University of Galați. Also, sincere appreciations to Ș.L. dr. phys. Alina Cantaragiu for SEM-EDX analyzes, to Prof. univ. dr. eng. Virgil Teodor for 2D roughness profiles and to dr. eng. Vasile Bașliu for the XRD analyzes.

I would also like to thank to my colleagues from CC-ITES for the offered support and my Ph.D collegues Laurenţiu Mardare and Nicoleta Simionescu for the moral support and encouragement advices.

Special thanks to my beloved parents Ion and Jenica and also, my brother Ionuţ that offered full moral and financial support during this period.

Last but not least, faithful gratitude to my other half, Adriana, for the unconditionally motivation, support and love in all this period in order to achieve the proposed objectives.

Finally, i wish to thank to all my friends for thier support and last but not least i gratitude God for the winsdom and strenght.

ec. Valentin Marian Dumitraşcu,
„Dunărea de Jos" University of Galaţi
April, 2018

# TABLE OF CONTENT

*** The numbering of chapter, figures, tables, formulas and references of the summary corresponds to PHD thesis numbering**

**Key words:**

**Functional surfaces, anodic oxidation, aluminum oxide, nanoporous aluminum oxide layers, corrosion, wear**

# INTRODUCTION

In the last years, functional surfaces have received an increased attention due to human complex and diversified needs and in order to obtain materials with improved properties regardless the environment where they are used and to require a low production and maintenance costs.

The aluminum oxide layers formed by anodic oxidation are used in numerous domains, being used as anticorrosive protection method and as method for building decoration and architecture, as method to improve the mechanical properties of aluminum and its alloys and as method to functionalization of aluminum and its alloys as templates to fabricate nanowires, nanotubes or nanoporous membranes.

The thesis approach the development of nanoporous aluminum oxide layers by anodic oxidation and assess the influence of imposed parameters in anodic oxidation process on the morphological, structural and compositional characteristics. Also, the influence of imposed parameters in the electrochemical process on anticorrosive, mechanical and wetting properties of the obtained nanoporous aluminum oxide layers was analyzed.

The PhD thesis entitled ***„Functional surfaces obtained by electrochemical methods and their characterization”*** can be structured in 3 parts: a theoretical part, an experimental research part and a part with the general conclusions, scientific contributions and future research directions, a total of **8 chapters**, **100 figures** and **22 tables**. Partial conclusions and bibliographical references are exposed at the end of each chapter.

In the chapter 1, entitled ***„Current trends on functional surfaces fabrication”*** it was conducted a bibliographic study which analyze the national and international research on functional surfaces and the study was focused on nanoporous aluminum oxide obtained by anodic oxidation method. Also, the results from scientific literature on the corrosion behavior of nanoporous aluminum oxide layers and the behavior under the mechanical factors are presented. At end of chapter 1 the research area, the aims and the experimental research program of PHD thesis are presented.

The experimental methods used, the results obtained and their interpretation are exposed in chapter 2, 3, 4, 5 and 6.

In chapter 2 entitled ***„Materials, methods and experimental techniques”*** are presented the materials used in experimental research, the methods used to prepare the substrate, the method used to grow nanoporous aluminum oxide layers and the methods and techniques used to characterize the nanoporous aluminum oxide layers properties.

Chapter 3 with the title ***„Influence of electrochemical parameters imposed in anodic oxidation process on nanoporous aluminum oxide layers characteristics”*** present the influence of the parameters (potential, time, electrolyte stirring rate) imposed in the anodic oxidation process on morphological, structural, compositional, thickness, 2D profilometry and wetting characteristics of nanoporous aluminum oxide layers obtained in $H_2SO_4$ 1 M in which was added 1 g/L $Al_2(SO_4)_3$ x 18 $H_2O$ at room temperature.

Within the chapter 4, entitled *„Influence of electrochemical parameters imposed in anodic oxidation process on anticorrosive properties of nanoporous aluminum oxide layers"* a comparative study between nanoporous aluminum oxide layers and aluminum Al1050 corrosion resistance has been achieved.

The anticorrosive properties of nanoporous aluminum oxide layers and aluminum Al1050 substrate were evaluated after immersion in 3.5% NaCl solution using electrochemical methods in DC and AC currents: open circuit potential, electrochemical impedance spectroscopy, potentiodynamic polarization and cyclic voltammetry. Also, the influence of parameters imposed in anodic oxidation process on the anticorrosive properties of the obtained nanoporous aluminum oxide layers was evaluated.

In chapter 5 with the title ***„The effect of electrochemical parameters imposed in anodic oxidation process on mechanical properties of nanoporous aluminum oxide layers"*** it is described the wear behavior of nanoporous aluminum oxide layers obtained by anodic oxidation in comparison with the wear behavior of aluminum Al1050 substrate. Also, it was analyzed the influence of imposed parameters on wear properties of nanoporous aluminum oxide layers using in-situ (friction coefficient) and ex-situ (SEM of wear tracks, volume of mass loss, wear rate) methods.

In chapter 6, entitled ***„The correlation between the electrochemical parameters imposed in anodic oxidation process with the wetting, corrosion and wear resistance properties of nanoporous aluminum oxide layers"*** are correlated the nanoporous aluminum oxide layers properties, highlighting the obtained layers that cumulate improved hydrophobic, anticorrosive and wear resistance properties, and also, the electrochemical parameters imposed in their fabrication processes.

Chapter 7, entitled ***„General conclusions, Perspectives and Future research direction"*** present the general conclusions on the experimental results on functional surfaces obtained by anodic oxidation on aluminum Al1050 surface.

Additionally, chapter 7 describes the future prospects for continuing the research on modification of aluminum Al1050 surface, research on tribocorrosive behavior of nanoporous aluminum oxide layers, research to evaluate the organic coatings adhesion on nanoporous aluminum oxide layers.

In chapter 8, with the title ***„Own contributions and Scientific achievements in the research domain"*** are exposed the original contributions, the scientific achievements which reflect the author originality in thesis domain by published scientific articles and participations to national and international conferences are acknowledged.

# CHAPTER 1.

# Current trends on functional surfaces fabrication

## 1.1. Functional surfaces

The developing of new materials or improving the properties of existing materials was always an interest for scientists. Since ancient times, peoples tried to improve material characteristics in order to increase their lifetime period or to be used in different domains.

In order to develop functional surfaces, the researcher's inspiration was the nature and they tried to discover and understand the basic principles of natural functional surfaces and to replicate them [1.1–1.5]. In order to develop functional materials and/or functional surfaces on classic materials, the research activities of scientists have been concentrating on preparation, characterization and developing of materials at a nanometric scale, under 100 nm.

In the last decades, the research activities have been focused on developing nanomaterials and nanotechnologies and also in knowledge transfer from research laboratory to industry. The developing of nanotechnologies and functional surfaces have increased industrial productivity, efficient usage of materials and energetic resources and reduced the impact of industrial and transportation pollution on environment and human health [1.14].

## 1.2. Fabrication of functional surfaces on aluminum and its alloys

Depending on the field of application, the modification of aluminum and its alloys surfaces could be done using different methods. The consolidation of aluminum alloys properties through surface enhancement develops a broader horizon of use.

Depending on the functional surface formation approach, the fabrication methods could be classified in two categories: bottom up methods and top-down methods [1.15].

Also, depending on precursor nature that could be used in functional surfaces production, the fabrication methods could be divided in two categories (figure 1.1): fabrication methods of functional surfaces that use gaseous precursors and fabrication methods of functional surfaces that use liquid precursors [1.16].

## 1.3. Fabrication of functional surfaces by anodic oxidation

The nanoporous aluminum oxide layers could be obtained by electrochemical etching

process of aluminum substrate (pure or alloyed), in a liquid environment (electrolyte), known as anodic oxidation process.

The aluminum substrate used as working electrode (anode) is immersed into electrolyte, parallel to an electrode (cathode) made from the same material or an inert material in contact with the electrolyte (platinum, graphite, lead, stainless steel, etc.) and under electrical field action the positive species from electrolyte ($H^+$) are moving to cathode that receives an electron and is converted to hydrogen gas, and the negative species are moving to the anode where the following reactions take place [1.22]:

$$2Al^{3+} + 3O^{2-} \rightarrow Al_2O_3 \quad (1.1)$$

or

$$2Al^{3+} + 3OH^- \rightarrow Al_2O_3 + 3H^+ + 6e^- \quad (1.2)$$

$$Al_2O_3 + 6H^+ \rightarrow 2Al^{3+}(aq) + 3H_2O \quad (1.3)$$

that lead to the formation and dissolution almost instantaneous of aluminum oxide.

Depending on the parameters involved in anodic oxidation process and especially the electrolyte nature, the morphology of aluminum oxide layers could be a barrier-type or a nanoporous-type (composed by an outer nanoporous film and inner barrier-type film).

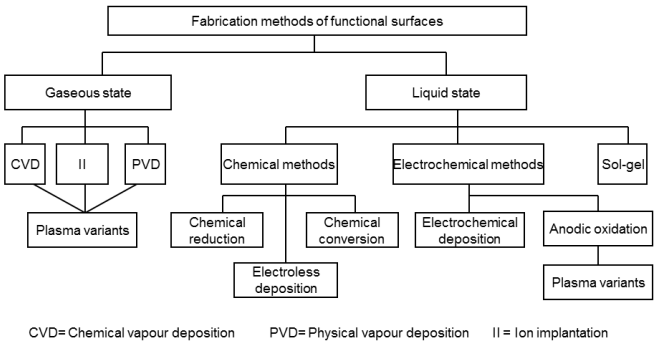


**Figure 1.1.** Fabrication methods of functional surfaces depending on precursors nature. Adaptation after [1.16]

Under the electrical field, the negative anions migrate to the anode, where the aluminum is positive charged due to electron loss. On anode surface, the chemical reactions take place at metal-aluminum oxide interface and also at aluminum oxide-electrolyte interface [1.26].

At metal-aluminum oxide interface, the oxygen anions are moving to the aluminum substrate according to the reaction:

$$2Al + 3O^{2-} \rightarrow Al_2O_3 + 6e^- \quad (1.4)$$

and at the aluminum oxide-electrolyte interface, the aluminum cations react with the water molecules:

$$2Al^{3+} + 3H_2O \rightarrow Al_2O_3 + 6H^+ \quad (1.5)$$

If the aluminum oxide layer is a porous-type, the aluminum substrate dissolution takes place according to the reaction:

$$2Al \rightarrow 2Al^{3+} + 6e^- \quad (1.6)$$

On cathode surface, an evolution of gaseous hydrogen takes place:

$$6H^+ + 6e^- \rightarrow 3H_2 \uparrow \quad (1.7)$$

The overall reaction of anodic oxidation process is:

$$2Al + 3H_2O \rightarrow Al_2O_3 + 3H_2 \quad (1.8)$$

## 1.4. Classification of aluminum oxide layers obtained by anodic oxidation

### 1.4.1. Barrier-type aluminum oxide layers

The barrier-type aluminum oxide layers are obtained when the anodic oxidation process takes place into an electrolyte that have a low interaction with the aluminum oxide: tartaric acid, organic acid electrolytes, etc. The barrier-type aluminum oxide layers usually have a uniform thickness on the entire surface due to the high efficiency of the imposed current in anodic oxidation process, with a negligible loss of aluminum ions into electrolyte.

The barrier-type aluminum oxide layers could be obtained by imposing of a constant potential or constant current during the anodic oxidation process (figure 1.2) [1.28]. Under galvanostatic conditions (constant current), the aluminum oxide layers grow in a constant electric field. In order to maintain the constant electric field, due to the increasing of electrical resistance of aluminum oxide layers, the voltage of electrochemical cell increase simultaneously with aluminum oxide thickness layers.

Under potentiostatic conditions, the recorded current evolution present a decreasing trend, until a steady state at a low value is reached. The current low value is influenced by the defects of aluminum oxide layer, which allow the passing of current to aluminum substrate or is influenced by the slow dissolution of aluminum oxide layer into electrolyte [1.29, 1.30].

The thickness of aluminum oxide layer is influenced by the voltage value imposed in anodic oxidation process and can be expressed in terms of nanometers per volt. The barrier-type layers of aluminum oxide present a grow rate of 1.2-1.4 nm/V [1.31].

### 1.4.2. Nanoporous-type aluminum oxide layers

The nanoporous aluminum oxide layers are intense studied due to their unique properties that allow to be used in different domains, from nanotechnology-based domains to different industrial or medical domains.

During the anodic oxidation processes that uses acid or basic electrolytes (that

dissolve the aluminum oxide such as sulphuric acid, oxalic acid, phosphoric acid, etc.), the nanoporous aluminum oxide layers are obtained.

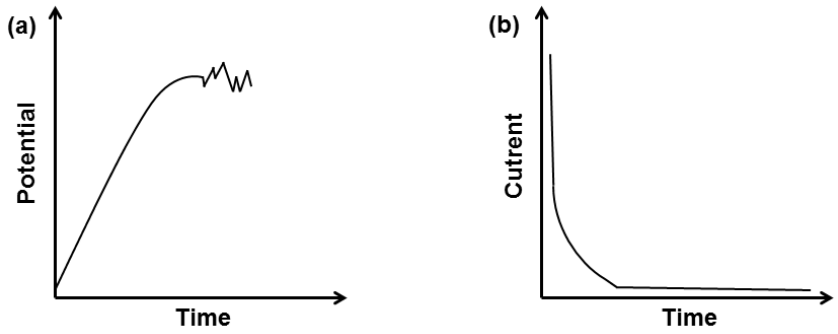


**Figure 1.2.** Schematic representation of potential and current evolution during the anodic oxidation process in (a) galvanostatic conditions and (b) potentiostatic conditions. Adapted after [1.28].

The nanoporous aluminum oxide layers have a complex structure, being composed by an outer porous structure with a high thickness at the electrolyte interface and a thin barrier-type structure at metal interface.

During the anodic oxidation processes a galvanostatic or potentiostatic regime could be used in order to obtain nanoporous aluminum oxide layers. The evolutions of potential-time and current-time diagrams are schematic exposed in figure 1.3 [1.48].

In the case of constant potential usage in anodic oxidation process, it can be seen that the current decrease rapidly from a high value to the minimum one followed by an increasing trend until the steady state is attained. The potential diagrams recorded during the anodic process at a constant current present an initial grow until a maximum value is reached and afterward following a decreasing trend.

During the anodic oxidation process, four stages of porous growth could be identified [1.48]:

- in the first stage, a barrier-type aluminum oxide layer growth in aluminum surface and under the aggressive electrolyte action, at aluminum oxide-electrolyte crevice-like structures (cracks) appear.
- in the second stage, due to electrolyte penetration through the cracks and resistance decreasing, the current flow to the aluminum substrate is allowed and aluminum ions are ejected to electrolyte. The cracks become nanopores once that the aluminum ions are ejected to the electrolyte.
- in the third stage the nanopores are ordered until the current or potential reach a steady state.
- in the fourth stage, the current or potential reach the steady state, the electric field action act on the barrier-type aluminum oxide layer from the pore bottom and the nanoporous aluminum oxide grow simultaneously with the anodic oxidation process duration [1.49].

The parameters imposed in anodic oxidation process and also the used electrolyte type influences the nanoporous aluminum oxide layer characteristics: diameter and pores density, layers thickness, etc.

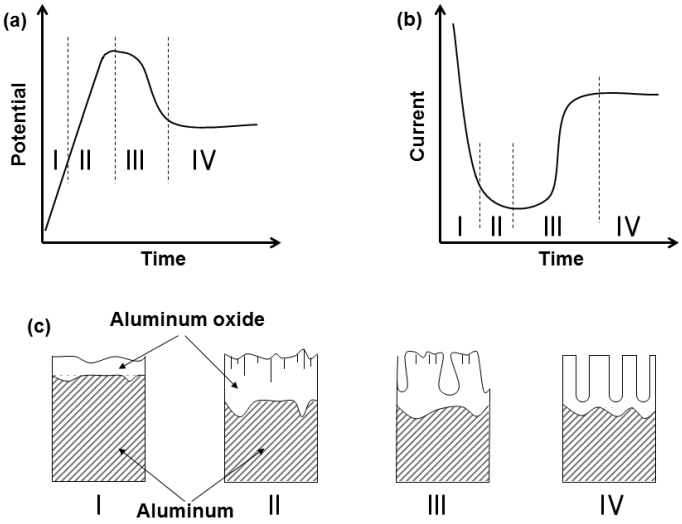


**Figure 1.3.** Schematic representation of potential and current evolutions during anodic oxidation process in (a) galvanostatic conditions and (b) potentiostatic conditions in order to obtain nanoporous aluminum oxide layers. (c) growing steps of nanoporous aluminum oxide layers. Adaptation after [1.48].

M.S. Hunter and P. Fowle [1.58] have determined a constant growth rate for the barrier-type aluminum oxide layer from the bottom of the pores during the anodic oxidation process. The growth rate of barrier-type layer from the bottom pores depend on the imposed potential in anodic oxidation process and are different for each electrolyte: the growth rate of barrier-type substrate in 15% sulphuric acid is 1 nm/V, for 4% phosphoric acid is 1.19 nm/V and for 2% oxalic acid is 1.18 nm/V.

In order to obtain ordered nanoporous aluminum oxide layers, different methods are used to order the nanopores: pretexturing, laser etching, nanoidentation with a mould, ion beam etching, but the most usual method is the anodic oxidation in two steps that involves reduced manufacturing costs. The accurate control of the imposed parameters in the anodic oxidation process lead to the fabrication of ordered nanoporous aluminum oxide layers.

## 1.5. Corrosion properties evaluation of aluminum oxide layers

Due to its position in reactivity scale, pure aluminum is a very reactive metal. A native aluminum oxide layer covers the aluminum after exposure to the air and offers an improved corrosion resistance. At room temperature, the thickness of native aluminum oxide is between 2.5 and 10 nm [1.75]. Aluminum and its alloys could be used in different environments, without supplementary protection relying only on the protection offered by the native aluminum oxide

According to Porboix diagram, the native aluminum oxide is stable and offer protection for the substrate as long as the electrolyte pH is between 4 and 8.5. In an acid

environment, with a pH lower that 4, aluminum is dissolved into aluminum ions and in a basic environment, with a pH grater than 8.5, aluminum is dissolved in aluminum oxide ions. In these situations, after the interaction with the environment (electrolyte), the aluminum corrosion takes place [1.29, 1.76].

Even if pure aluminum presents an improved corrosion resistance, the aluminum alloys, due to intermetallic particles formed on their surfaces could present local corrosion forms. The occurrence of local corrosion is caused by two factors: the electrolyte type, chemical and metallographic structure of material.

Among all localized corrosion phenomenon, the pitting corrosion affects aluminum and its alloys, being the most common corrosion form.

Pitting corrosion appears in heterogeneous area from aluminum and its alloys surfaces: grains boundaries, defects, inclusions and material dislocations. Pitting corrosion initially appears at aluminum oxide-electrolyte interface and after that it migrates through the aluminum oxide layer to the metallic substrate.

In order to improve the corrosion resistance of aluminum and its alloys, different protection methods have been used:

- conversion coatings;
- organic coatings;
- thin films obtained by atomic deposition;
- anodic oxidation.

### 1.5.1. Conversion coatings

The conversion coatings are used as intermediate coatings between aluminum substrate and organic coatings or as anticorrosion coatings.

### 1.5.2. Organic coatings

Organic coatings offer anticorrosive properties both by forming an active protection barrier on metal surface and by releasing of pigments into electrolyte that act as inhibitor agents [1.89].

### 1.5.3. Thin films obtained by atomic deposition

The fabrication of thin films by atomic deposition assumes the substrate exposure to different gaseous precursors in a sequential mode and for a controlled duration [1.91, 1.92]. The advantages of thin films fabrication by atomic deposition with anticorrosive properties are: rigorous control of thickness and films composition, low defects number, high reproducibility and films uniformity.

### 1.5.4. Anodic oxidation

The anodic oxidation process involves the formation of an aluminum oxide layers at the metal-electrolyte interface, with variable thickness that offers improved properties to the substrate and especially an improved anticorrosive resistance.

The corrosion assays have revealed an increased anticorrosion resistance of aluminum oxide layers, regardless of their structures: barrier-type or nanoporous-type aluminum oxide layers. Even if the nanoporous aluminum oxide layers are penetrated by the aggressive electrolyte, the barrier-type layer from the bottom of pores protects the aluminum substrate.

## 1.6. Wear resistance evaluation of aluminum oxide layers

Tribology is the sciences that study the wear phenomena between two or more surfaces in contact and in relative motion [1.16].

The tribological properties of functional surfaces are influenced by the surface nature and the surface roughness and also by following factors:

- contact pressure and normal force;
- sliding velocity of the surfaces;
- environment conditions (temperature, humidity, etc.);
- motion nature (continuous, periodic).

The anodized aluminum and its alloys are used usually in aeronautics and transport that replaces the steel pieces that present a high weight and involve expensive costs.

The nanoporous aluminum oxide layers are used in tribological applications because of their porous structure that could be used as nano-reservoirs for liquid lubricants or template for solid lubricants [1.101, 1.102].

H. Kim and his team [1.104] have investigated the wear behavior of nanoporous aluminum oxide layers obtained by anodic oxidation in sulphuric acid at 25 V, oxalic acid at 40 V and phosphoric acid at 195 V using a bidirectional sliding movement with a 440C steel ball and applied 4 normal forces between 1 mN and 1 N. They observed that the formed nanopores diameter in aluminum oxide layer have an important roll on the mechanical properties of the obtained layers. The increasing of nanopores diameters cause a decreasing of layer wear resistances and an increasing of friction coefficient between steel ball and aluminum oxide layers. Also, the applied normal forces in wear tests cause a decreasing of friction coefficients because of the thin and smooth tribolayers that are formed on the aluminum oxide layers due to tribochemical reaction and the wear debris.

The increasing of anodic oxidation duration in sulphuric acid lead to the increasing of porosity and decreasing of aluminum oxide layers thickness (due to dissolution under the electrical field). The nanoidentation values of nanoporous aluminum oxide layers present a reverse proportionality with the anodic oxidation process duration [1.110].

## 1.7. Partial conclusions

In the last decades, the research on functional surfaces domains have concern an increased number of scientists, and their studies to develop new functional surfaces with novel properties.

The aluminum and its alloys have received an increased attention due to their intrinsic properties and due to the new properties that are offered by the functional surfaces and could be used in different domains: from transport to aeronautics, from medicine to energy production or communications.

The functional surfaces on aluminum and its alloys could be fabricated using different methods, but the most usually method is anodic oxidation.

Into the anodic oxidation process, external parameters are imposed during electrochemical process and their variations allow a rigorous control of morphological and functional structure of aluminum oxide layers grow on aluminum and its alloys surfaces. Other advantages of anodic oxidation process are the low cost of functional surface fabrication (equipments costs or electrolytes), fabrication of functional surfaces on irregular supports, increased adherence of functional surfaces to aluminum substrate, industrial applications of the anodic oxidation method and of functional surfaces obtained.

The formation mechanism of aluminum oxide layers by anodic oxidation consist in electrolyte molecules dissociation and their transport under the electric field influence to the anode, where a reaction with the aluminum ions expulsed from the substrate take place and the aluminum oxide layer is formed on aluminum surface. The nanoporous aluminum oxide layers are formed in acid electrolytes which cause a partial dissolution of aluminum oxide and the nanoporous structure at the aluminum oxide-electrolyte interface is formed.

The functional surfaces obtained by anodic oxidation improve the physico-chemical and mechanical properties of aluminum substrate.

## 1.8. Aims and research directions

- Conducting a bibliographic study on current national and international trends on functional surfaces developed by electrochemical methods on aluminum and its alloys.
- The investigation of aluminum oxide layers forming mechanism on aluminum and its alloys by anodic oxidation process.
- The optimization of applied parameters in order to obtain nanoporous aluminum oxide layers on 1050 aluminum alloy.
- Fabrication of nanoporous aluminum oxide layers by anodic oxidation process on 1050 aluminum alloy surface.
- Morphological, compositional and structural characterization of nanoporous aluminum oxide layers.
- Thickness measurements of nanoporous aluminum oxide layers using scanning electron microscopy.
- Determination of 2D roughness profiles and wetting properties of nanoporous aluminum

oxide layers.
- Evaluation of corrosion behavior of nanoporous aluminum oxide layers immersed in 3.5% NaCl solution, an aggressive environment that simulate the aggression of marine environment, using electrochemical methods such as: open circuit potential (OCP), electrochemical impedance spectroscopy (EIS), potentiodynamic polarization (PD) and cyclic voltammetry (CV).
- Evalutaion of wear properties of nanoporous aluminum oxide layers by determination of friction coefficient and wear volume.
- Wear tracks characterization using scanning electron microscopy and 2D roughness profiles.
- Correlation of nanoporous aluminum oxide characteristics with the variation of imposed parameters in anodic oxidation process.
- Results disseminations and the transfer of obtained knowledges to the industry.

## 1.9. Experimental research program

The experimental research program was conductes in the research laboratory of Competence Center Interface-Tribocorrosion and Electrochemical Systems (CC-ITES) and Research and Development Center for Thermoset Composites (CDCOMT) from „Dunărerea de Jos" University of Galați.

In the Competence Center Interface-Tribocorrosion and Electrochemical Systems (CC-ITES) research laboratory the following stages of experimental were conducted:
- Preparation of solutions used in electrochemical polishing, anodic oxidation and corrosion processes.
-Al1050 samples preparation, which were used as support for nanoporous aluminum oxide growth, (cutting, cleaning, mechanical polishing, electrochemical polishing, resin isolation, etc).
- Fabrication of nanoporous aluminum oxide layers varying the potential and anodic oxidation process duration and also the electrolyte stirring rate during the electrochemical process.
- Corrosion behavior evaluation of nanoporous aluminum oxide layers using electrochemical methods such as: open circuit potential, electrochemical impedance spectroscopy, potentiodynamic polarization and cyclic voltammetry.
- Evaluation of nanoporous aluminum oxide layer wetting properties using distilled water droplets.

In the Research and Development Center for Thermoset Composites (CDCOMT) laboratory, the following experimental research stages were conducted:
- Morphological, compositional and structural characterization of nanoporous aluminum oxide layers.
- Evaluation of nanoporous aluminum oxide layers wear behavior using in-situ and ex-situ methods.
- Determination of nanoporous aluminum oxide layers and wear tracks roughness profiles.

## 1.10. Selective references from chapter 1

[1.1] X. Yao, Y. Song, L. Jiang, Applications of bio-inspired special wettable surfaces, Advances Materials, 23, (2011), 719 – 734, DOI: 10.1002/adma.201002689
[1.2] H. Yang, F. Liang, Y. Chen, Q. Wang, X. Qu, Z. Yang, Lotus leaf inspired robust superhydrophobic coating from strawberry-like Janus particles, NPG Asia Materials, 7, (2015), e176, DOI: 10.1038/am.2015.33
[1.3] S.S. Latthe, A.B. Gurav, C.S. Maruti, R.S. Vhatkar, Recent progress in preparation of superhydrophobic surfaces: a review, Journal of Surface Engineered Materials and Advanced Technology, 2, (2012), 76 – 94, DOI: 10.4236/jsemat.2012.22014
[1.4] Z. Guo, W. Liu, B.-L. Su, Superhydrophobic surfaces: From natural to biomimetic to functional, Journal of Colloid and Interface Science, 353, (2011), 335 – 355,
DOI: 10.1016/j.jcis.2010.08.047
[1.5] S. Shin, J. Seo, H. Han, S. Kang, H. Kim, T. Lee, Bio-inspired extreme wetting surfaces for biomedical applications, Materials, 9, (2016), 116 - 142, DOI:10.3390/ma9020116
[1.14] M.C. Roco, W.S. Bainbridge, Societal implications of nanoscience and nanotechnology: Maximizing human benefit, Journal of Nanoparticle Research, 7, (2005), 1 – 13, DOI: 10.1007/s11051-004-2336-5
[1.15] A. Biswas, I.S. Bayer, A.S. Biris, T. Wang, E. Dervishi, F. Faupel, Advances in top-down and bottom-up surface nanofabrication: Techniques, applications & future prospects, Advances in Colloid and Interface Science, 170, (2012), 2 – 27,
DOI: 10.1016/j.cis.2011.11.001
[1.16] K. Holmberg, A. Matthews, Coatings tribology, properties, mechanisms, techniques and applications in surface engineering 2nd Edition, Elsevier, Amsterdam, Olanda, 2009, ISBN: 978-0-444-52750-9
[1.22] X. Qin, J. Zhang, X. Meng, C. Deng, L. Zhang, G. Ding, H. Zeng, X. Xu, Preparation and analysis of anodic aluminum oxide films with continuously tunable interpore distances, Applied Surface Science, 328, (2015), 459 – 465, DOI: 10.1016/j.apsusc.2014.12.048
[1.26] Marloes van Put, Teză de disertație, Potentiodynamic anodizing and adhesive bonding of aluminum for the aerospace industry, Delft University of Technology, 2013,
https://repository.tudelft.nl/islandora/object/uuid:19144038-253f-46fd-aac8-ce58208d8a8a?collection=education, (accesat în data de 4 ianuarie 2018)
[1.28] T. Aerts, I. De Graeve, H. Terryn, Anodizing of aluminium under applied electrode temperature:Process evaluation and elimination of burning at high current densities, Surface and Coatings Technology, 204, (2010), 2754 – 2760, DOI: 10.1016/j.surfcoat.2010.02.031
[1.29] P.G. Sheasby, R. Pinner, The surface treatment and finishing of aluminum and its alloys, 6th Edition, Finishing Publications Ltd. and ASM International, 2001,
ISBN: 0-904477-21-5
[1.30] G.E. Thompson, Porous anodic alumina: fabrication, characterization and applications, Thin Solid Films, 297, (1997), 192 – 201, DOI: 10.1016/S0040-6090(96)09440-0
[1.31] J.P. O'Sullivan, G.C. Wood, The morphology and mechanism of formation of porous anodic films on aluminium, Proceedings of the Royal Society A, 317, (1970), 511 – 543,
DOI: 10.1098/rspa.1970.0129

[1.48] V.P. Parkhytik, V.I. Shershulsky, Theoretical modeling of porous oxide growth on aluminium, IOP Series: Journal of Physics D: Applied Physics, 25, (1992), 1258, ISSN: 1361-6463, http://iopscience.iop.org/article/10.1088/0022-3727/25/8/017/meta (accesat în data de 8 ianurie 2018)
[1.49] G.D. Sulka, Highly ordered anodic porous alumina formation by self-organized anodizing, Chapter 1 in Nanostructured Materials in Electrochemistry, ed. A. Eftekhari, Wiley-VCH Verlag GmbH & Co. KGaA, 2008, DOI: 10.1002/9783527621507.ch1
[1.58] M.S. Hunter, P. Fowle, Determination of barrier layer thickness of anodic oxide coatings, Journal of the Electrochemical Society, 101, (1954), 481 – 485,
DOI: 10.1149/1.2781304
[1.65] H. Asoh, K. Nishio, M. Nakao, T. Tamamura, H. Masuda, Conditions for fabrication of ideally ordered anodic porous alumina using pretextured Al, Journal of the Electrochemical Society, 148, (2001), B152 – B156, DOI: 10.1149/1.1355686
[1.66] S. Shingubara, Y. Murakami, K. Murimoto, T. Takahagi, Formation of aluminum nanodot array by combination of nanoidentation and anodic oxidation of aluminum, Surface Science, 532-535, (2003), 317 – 323, DOI: 10.1016/S0039-6028(03)00433-3
[1.67] K.R. Zavadil, J.A. Ohlhausen, P.G. Kotula, Nanoscale void nucleation and growth in the passive oxide on aluminum as a prepitting process, Journal of the Electrochemical Society, 153, (2006), B296 – B303, DOI: 10.1149/1.2207739
[1.68] A.P. Robinson, G. Burnell, M. Hu, J.L. MacManus-Driscoll, Controlled, perfect ordering in ultrathin anodic aluminum oxide templates on silicon, Applied Physics Letters, 91, (2007), 143123, DOI: 10.1063/1.2794031
[1.75] V.F. Henley, Anodic oxidation of aluminium and its alloys, Pergamon Press, Oxford, Anglia, 1982, ISBN: 9781483147338
[1.76] N.L. Sukiman, X. Zhou, N. Birbilis, A.E. Hughes, J.M.C. Mol, S.J. Garcia, X. Zhou, G.E. Thompson, Chapter 2: Durability and Corrosion of aluminium and its alloys: Overview, property space, techniques and developments, in Aluminium alloys – new trends in fabrication and applications, Ed. Z. Ahmad, InTech, 2012, ISBN: 978-953-51-0861-0,
DOI: 10.5772/53752
[1.89] S.B. Lyon, R. Bingham, D.J. Mills, Advances in corrosion protection by organic coatings: What we know and what we would like to know, Progress in Organic Coatings, 102, (2017), 2 – 7, DOI: 10.1016/j.porgcoat.2016.04.030
[1.91] S.M. George, Atomic Layer Deposition: An overview, Chemical Reviews, 110, (2010), 111 – 131, DOI: 10.1021/cr900056b
[1.92] R.L. Puurunen, Surface chemistry of atomic layer deposition: A case study for the trimethylaluminum/water process, Journal of Applied Physics, 97, (2005), 121301,
DOI: 10.1063/1.1940727
[1.101] T. Kmita, M. Bara, Surface oxide layers with an increased carbon content for applications in oil-less tribological systems, Chemical and Process Engineering, 33, (2012), 479 – 486, ISSN: 2300-1925, DOI: 10.2478/v10176-012-0040-z
[1.102] Y. Wang, L. Xia, J. Ding, N. Yuan, Y. Zhu, Tribological behaviors of lubricants modified nanoporous anodic alumina film, Tribology Letters, 49, (2013), 431 – 437,
DOI: 10.1007/s11249-012-0086-6

[1.104] H. Kim, D. Kim, W. Lee, S.J. Cho, J.-H. Hahn, H.-S. Ahn, Tribological properties of nanoporous anodic aluminum oxide film, Surface and Coatings Technology, 205, (2010), 1431 – 1437, DOI: 10.1016/j.surfcoat.2010.07.056
[1.110] A. Belwalkar, E. Grasing, W. Van Geertryden, Z. Huang, W.Z. Misiolek, Effect of processing parameters on pore structure and thickness of anodic aluminum oxide (AAO) tubular membranes, Journal of Membrane Science, 319, (2008), 192 – 198,
DOI: 10.1016/j.memsci.2008.03.044

# CHAPTER 2.

# Materials, methods and experimental techniques

In chapter 2, the support materials, the methods used to prepare the 1050 aluminum substrate and the solutions, as well the experimental procedures used to obtain the nanoporous aluminum oxide layers are described. The methods and equipments used for nanoporous aluminum oxide layers in-situ and ex-situ characterization are presented, also.

## 2.1 Materials

### 2.1.1. Aluminum and its alloys

Aluminum is the third most common chemical element, after oxygen and silicon in earth's crust, but not in a pure form, usually as aluminum compounds such as bauxite [2.2]. Aluminum is abbreviated with the chemical symbol Al, has an atomic number equal with 13, that means it has on the outer layer 3 electrons and the valence equal with 3, which offer a high reactivity especially with the oxygen.

The 1050 aluminum alloy known as commercial pure aluminum is included in the first family of aluminum alloys that mean it has a high purity equal with 99.5%. The 1050 aluminum alloy is a soft and ductile material and the alloying elements or impurities are iron and silicon. Due to the impurities and the rolling process, the commercial pure aluminum gains an increased strength and usually is produced as aluminum sheets. The 1050 aluminum alloy become ductile after the thermal treatment and present a high corrosion resistance being the right choice for pipes fabrication, as packaging used in food or chemical industries, but it can be used for car panels fabrications where the elongation rate is an important factor in their utilization process.

### 2.1.2. Aluminum oxide

The aluminum oxide (alumina, $Al_2O_3$) is one of the simplest covalent oxides in comparison with other ceramic materials and show improved thermal, physical and chemical properties [2.7]. The aluminum oxide structure could be a crystalline one, a polycrystalline or amorphous one, depending on the fabrication method [2.8].

From the many fabrication methods of aluminum oxide layers (barrier-type or porous-type), the anodic oxidation process fascinated the researchers due to high versatility, lower

equipment costs and physical, mechanical and anti-corrosive properties of obtained aluminum oxide layers.

Depending on the involved parameters in the anodic oxidation process, two different types of aluminum oxide layers could be obtained: a barrier-type layer (figure 2.1) or a porous-type layer (figure 2.2) [2.18]. The barrier-type aluminum oxide layers are obtained due to the slow reactivity with the electrolyte during the anodic oxidation process [2.18]. The barrier-type aluminum oxide layers are obtained into electrolytes with a neutral or basic pH. Their important characteristics are: hardness, wear resistance and electrical isolator. Also, the barrier-type aluminum oxide layers show improved anti-corrosive properties because it acts as a barrier against aggressive ions and offer protection to the aluminum substrate [2.18].

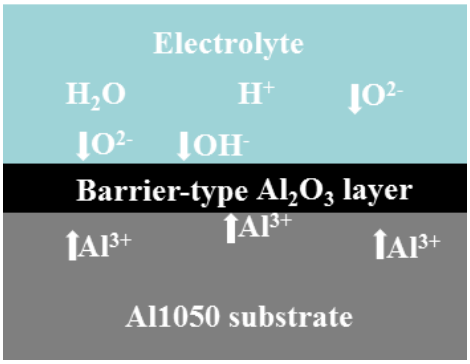


**Figure 2.1.** Schematic representation of barrier-type aluminum oxide layers obtained by anodic oxidation. Adaptation after [2.18]

The porous or nanoporous aluminum oxide layers have an outer porous structure and an inner stable barrier-type thin film [2.18, 2.22]. The porous aluminum oxide layers are obtained after the anodic oxidation of aluminum substrate in acid electrolytes (sulphuric acid [2.14, 2.17], oxalic acid [2.23], and phosphoric acid [2.24], etc.) that react with the aluminum oxide layer and cause a partial dissolution.

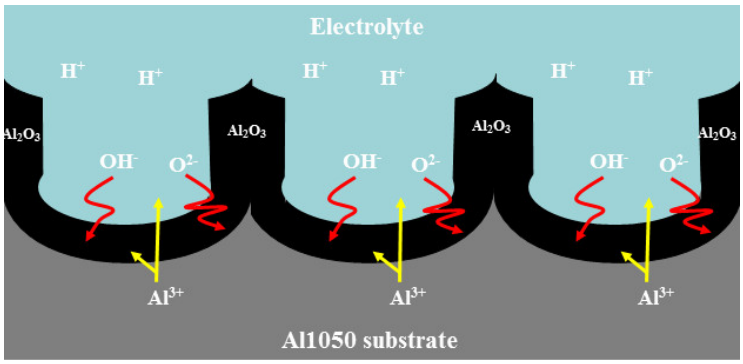


**Figure 2.2.** Schematic representation of nanoporous aluminum oxide layers obtained by anodic oxidation. Adaptation after [2.18].

Due to the unique properties, the nanoporous aluminum oxide layers are used in different industries, from the nanotechnology domains where are used for sensors fabrication or templates to obtain nanowires or nanotubes, etc. with various length [2.26, 2.27], until the anti-corrosive surfaces with a complex structure [2.28], from the wastewater treatment domain to the medical domain where are used as supports for cell grown in incubators [2.27, 2.29].

## 2.2. Electrochemical methods for 1050 aluminum alloy surface modification

### 2.2.1. 1050 aluminum alloy surface preparation

The 1050 aluminum alloy (Al1050, 99.5%) it was used as substrate for nanoporous aluminum oxide grown using electrochemical methods. The 1050 aluminum alloy sheet was cut in pieces with 2 x 30 x 35 mm dimensions using a guillotine and after that the pieces were mechanical polished with abrasive paper, with different granulation, in order to remove the macroscopic defects and the native aluminum oxide film.

The mechanical polished Al1050 samples were washed with distilled water and chemical cleaned by NaOH immersion, washed in water for 60 seconds, rinsed with distilled water for 30 seconds, dried in an oven under hot air and after that were stored in a desiccator.

### 2.2.2. Electrochemical polishing of 1050 aluminum alloy

The 1050 aluminum alloy samples were electrochemical polished in an electrolyte of 15% $Na_2CO_3$ and 5% $Na_3PO_4$ in order to remove all the impurities remains on their surfaces after the mechanical polish process. The electrochemical cell used in the electrochemical polishing process was formed by 2 electrodes (an anode and a cathode). The 1050 aluminum alloy samples with active surface of 6.5 $cm^2$ were used as anode and a 1050 aluminum alloy piece with an active surface of 7.54 $cm^2$ was used as cathode. The both 1050 aluminum alloy samples were immersed into electrolyte, with parallel active surfaces and after that with 2 electric grippers they were connected to an external high power source (TDK LAMBDA GEN 300–8).

The electrochemical polishing processes were done at a potential value of 2 V and a temperature of 80$^oC$. After the electrochemical polishing process, the 1050 aluminum alloy samples were rinsed with distilled water, dry in oven under hot air and stored in a desiccator until the next process.

### 2.2.3. Anodic oxidation of 1050 aluminum alloy

The anodic oxidation process produces a nanoporous aluminum oxide layer on 1050 aluminum alloy surface. The electrochemical polished 1050 aluminum alloy samples were subjected to anodic oxidation process, under a potentiostatic regime, in 1 M $H_2SO_4$ electrolyte in which was added 1 g/L $Al_2(SO_4)_3$ x 18 $H_2O$ in order to simulate an aged electrolyte. The

involved parameters in the anodic oxidation process (potential, time and electrolyte stirring rate) were varied in order to observe their influence on morphological, compositional and structural characteristics and on physical, mechanical and chemical properties of nanoporous aluminum oxide layers obtained.

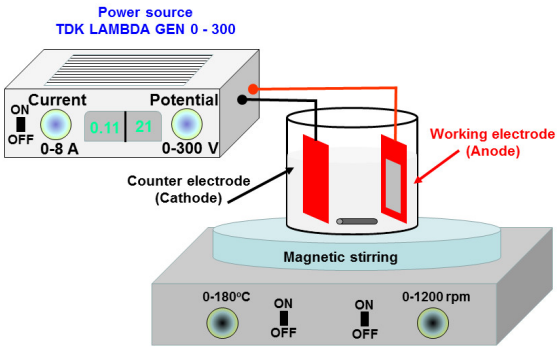


**Figure 2.5.** Experimental set-up used in anodic oxidation processes

The anodic oxidation processes were conducted in a classical electrochemical cell, presented in figure 2.5, where the electrochemical polished Al1050 sample, with an active surface of 4 $cm^2$ was used as anode. As cathode a 1050 aluminum alloy sample was used with an active surface of 12 $cm^2$. Both 1050 aluminum alloy samples were immersed into 200 mL electrolyte and using 2 electric grippers were connected to an external high power source (TDK LAMBDA GEN 300-8).

In order to obtain nanoporous aluminum oxide layers with a uniform cellular structure, the imposed parameters in the anodic oxidation process were ranged accordingly: the potential was ranged between 1 and 25 V, the anodic oxidation process duration was ranged between 10 and 480 minutes and the electrolyte stirring rate was varied between 0 and 700 rpm.

## 2.3. Experimental techniques used for nanoporous aluminum oxide layers characterization

The morphological, compositional and structural characterization of nanoporous aluminum oxide layers were done in the research laboratory of „Dunărea de Jos" University of Galați. The wetting properties and the corrosion behavior were evaluated in the research laboratory of Competence Center Interfaces-Tribocorrosion and Electrochemical Systems.

The wear resistance of nanoporous aluminum oxide layers was evaluated with the equipments from Research and Development Center for Thermoset Composites (CDCOMT) laboratory.

### 2.3.1. Morphological and compositional characterization

The morphological characterization of nanoporous aluminum oxide layers obtained by anodic oxidation on top-view and cross-section were done using the scanning electron microscope (SEM) FEI QUANTA 200 from „Dunărea de Jos" University of Galați. Using a disperse X-ray analyzer, the compositional analyzes of nanoporous aluminum oxide layers were performed.

### 2.3.2. Structural characterization

Using X-ray diffraction method and the Dron-3 equipment from „Dunărea de Jos" University of Galați, the structural characterization of obtained nanoporous aluminum oxide layers by anodic oxidation were carried out. The XRD diffractograms were recorded using a Molybdenum anode (Mo, $\lambda_{Ka}$=0.71073 Å). The values were analyzed using MATCH 3 software connected to an open access data base Crystallography Open Database (COD).

### 2.3.3. Roughness

The 2D roughness profiles were recorded using the Mytutoyo Surftest SJ-210 Series contact-type roughness tester by moving the stylus tip on nanoporous aluminum oxide layer surfaces for 2.5 mm with the speed of 0.5 μm/s.

### 2.3.4. Wetting properties

The evaluation of contact angles values between the analyzed surfaces and water droplets were carried out using the goniometer OCA 15 EC, Dataphysics, Germany, connected to a PC and the experimental data were recorded with SCA20 software.

The 1050 aluminum alloy surfaces were fixed on the working table of equipment, under the syringe needle (filed with distilled water) that was connected to a controlled by PC dosing system. The droplets volume settled on analyzed surfaces were around 5 μL. After the droplets touch the analyzed surfaces, the droplets profiles were photographed and using Young-Laplace method were fitted in order to obtain the mean value of contact angles.

### 2.3.5. Corrosion behavior of nanoporous aluminum oxide layers

The corrosion behavior of electrochemical polished 1050 aluminum alloy surface and nanoporous aluminum oxide layers were evaluated in Electrochemistry and Corrosion laboratory, Competence Center Interfaces-Tribocorrosion and Electrochemical Systems from „Dunărea de Jos" University of Galați.

The corrosion behavior of electrochemical polished and anodized 1050 aluminum alloy samples were evaluated using 3.5% NaCl solution with a pH = 5.75 (which simulate the aggressive behavior of marine environment) in order to evaluate the influence of imposed parameters in anodic oxidation process on anticorrosive properties of nanoporous aluminum

oxide layers.

The samples subjected to corrosion were connected to a copper wire and isolated with epoxy resin to obtain an active surface of 1.6 $cm^2$. The electrochemical cell presented in figure 2.13 was composed by an inert glass recipient with a volume of 150 mL, in which the electrolyte was added, and after that the counter electrode (Pt-Rh grid), the reference electrode Ag/AgCl (KCl saturated, +199 mV vs. NHE) and the working electrode, electropolished or anodized 1050 aluminum alloy samples were immersed. The electrochemical cell was connected to a potentiostat/galvanostat VoltaLab PGZ301 and the experimental data were recorded with Voltamaster 4.0 software.

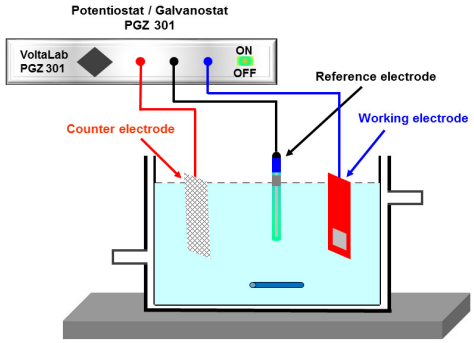


**Figure 2.13.** Experimental set-up used in corrosion assays.

The experimental protocol used to evaluate the corrosion resistance was composed by the following electrochemical methods:

- open circuit potential, measured for 17 hours;
- electrochemical impedance spectroscopy versus free potential, in the frequency domain: $10^5$ Hz – $10^1$ Hz, using a sinusoidal signal with an amplitude of 10 mV;
- coulometry;
- potentiodynamic polarization diagrams in a range of potential between -1.45 V vs. Ag/AgCl to -0.4 V vs. Ag/AgCl with a scan rate of 1 mV/s.
-cyclic voltammetry diagrams recorded with a scan rate of 1 mV/s in a potential range between -1.45 V vs. Ag/AgCl şi -0.4 V vs. Ag/AgCl.

## 2.3.6. Wear behavior of nanoporous aluminum oxide layers

The wear behavior of nanoporous aluminum oxide layers were evaluated using TRM 1000 tribometer from Research and Development Center for Thermoset Composites (CDCOMT), „Dunărea de Jos" University of Galați using pin-on-disk configuration. The tribometer was connected to a computer and data were recorded with Tribo Control V9 software.

During the wear test, as pin was used an alumina ball, grade 10, and a diameter of 10 mm (Ceratec, Netherlands), and as disks were used the electrochemical polished or anodized 1050 aluminum alloy surfaces.

In order to evaluate the wear resistance of electrochemical polished and anodized 1050

aluminum alloy surfaces, the wear tests were done by applying 5 N normal force for 50 minutes and a rotation speed of 9.55 rpm The wear tracks formed on the analyzed surfaces were evaluated using the roughness tester Mytutoyo Surftest SJ-210 Series and the scanning electron microscope FEI QUANTA 200.

## 2.4. Partial conclusions

In chapter 2 the methods used in nanoporous aluminum oxide layers fabrication and the steps that were taken until the anodic oxidation process were presented and the equipment used to evaluate the nanoporous aluminum oxide characteristics, also.

The 1050 aluminum alloy samples were mechanical polished, chemical cleaned and electrochemical polished in order to obtain smooth surfaces, on which nanoporous aluminum oxide layers will be grown by anodic oxidation in 1 M $H_2SO_4$ in which was added 1 g/L $Al_2(SO_4)_3$ x 18 $H_2O$.

The top-view and cross-section morphological characterization and chemical composition of nanoporous aluminum oxide layers were evaluated using scanning electron microscope coupled with an X-ray analyzer. The structural characterization of nanoporous aluminum oxide layers was realized using X-ray diffraction method and the roughness characterization was done using a contact-type roughness tester. Also, the influence of nanoporous aluminum oxide fabrication parameters on wetting, anti-corrosive and wear properties was evaluated.

The anodic oxidation process changes the morphological, compositional, structural and roughness properties of 1050 aluminum alloy samples which improve their wetting, anti-corrosive and wear characteristics. The equipments and the in-situ and ex-situ methods offer detailed information about the properties of nanoporous aluminum oxide layers obtained by anodic oxidation and offer information about the influence of imposed parameters into anodic oxidation process.

## 2.5. Selective references of Chapter 2

[2.2] N.N. Greenwood, A. Earnshaw – Chemistry of the elements, A doua Ediție, Capitolul 7: Aluminiul, Galiul, Indiul şi Taliul, Butterworth-Heinemann, Oxford, Anglia, 1997, ISBN: 978-0-7506-3365-9

[2.7] S.K. Lee, S.B. Lee, S.Y. Park, Y.S. Yi, C.W.Ahn, Structure of amorphous aluminum oxide, Physical Review Letters, 103, (2009), 095501-1 – 095501-4, DOI: 10.1103/PhysRevLett.103.095501

[2.8] T. Shirai, H. Watanabe, M. Fuji, M. Takahashi, Structural propertirs and surface Characteristics on aluminum oxide powders, Annual report of the Ceramics Research Laboratory Nagoya Institute of Technology, 9, (2009), 23 – 31, http://id.nii.ac.jp/1476/00002232/ (accesat în data de 24 decembrie 2017).

[2.14] **V.M. Dumitrascu**, L. Benea, Improving the corrosion behaviour of 6061 aluminum alloy by controlled anodic formed oxide layer, Revista de chimie (Bucuresti), 68, (2017), 77 – 80, http://www.revistadechimie.ro/article_eng.asp?ID=5393 (accesat în 24 decembrie 2017).

[2.17] H. Masuda, K. Yada, A. Osaka, Self-ordering of cell configuration of anodic porous alumina with large-size pores in phosphoric acid solution, Japanese Journal of Applied Physics, 37, (1998), L1340 – L1342, http://iopscience.iop.org/article/10.1143/JJAP.37.L1340 (accesat în 24 decembrie 2017).

[2.22] J.W. Diggle, T.C. Downie, C.W. Goulding, Anodic oxide films on aluminum, Chemical Reviews, 69, (1969), 365 – 405, DOI: 10.1012/cr60259a005

[2.23] M. Mohajeri, H. Akbarpour, Kowledge-based prediction of pore diameter of nanoporous anodic aluminum oxide, Journal of Electroanalytical Chemistry, 705, (2013), 57 – 63, DOI: 10.1016/j.elechem.2013.07.026

[2.24] M. Schenider, K. Krammer, The effect of bath aging on the microstructure of anodic oxide layers on AA1050, Surface and Coatings Technology, 246, (2014), 64 – 70, DOI: 10.1016/j.surfcoat.2014.03.008

[2.26] J. Ferre-Borrull, J. Pallares, G. Macias, L.F. Marsal, Nanostructural engineering of nanoporous anodic alumina for biosensing applications, Materials, 7, (2014), 5225 – 5253, DOI: 10.3390/ma7075225

[2.27] A.M.M. Jani, D. Losic, N.H. Voelcker, Nanoporous anodic aluminium oxide: Advances in surface engineering and emerging applications, Progress in Materials Science, 58, (2013), 636 – 704, DOI: 10.1016/j.pmatsci.2013.01.002

[2.28] Y. Zuo, P.-H. Zhao, J.-M. Zhao, The influences of sealing methods on corrosion behavior of anodized aluminum alloys in NaCl solutions, Surface and Coatings Technology, 166, (2003), 237 – 242, DOI: 10.1016/S0257-8972(02)00779-X

[2.29] D. Bruggemann, Nanoporous aluminium oxide membranes as cell interfaces, Journal of Nanomaterials (Hindawi Publishing Corporation), 2013, ID 460870, 18 pagini, DOI: 10.1155/2013/460870

[2.30] **V. Dumitrascu**, L. Benea, Influence of the anodic oxidation treatment on the corrosion behaviour of aluminium and aluminium alloys, The Annals of „Dunarea de Jos" University of Galaţi, Fascicle IX. Metallurgy and Materials Science, No. 3 – 2015, ISSN 1453 – 083X, http://www.fascicula9.ugal.ro/uploads/pdf/A2_3_2015.pdf (accesat în 24 decembrie 2017)

# CHAPTER 3.

# Influence of electrochemical parameters imposed in anodic oxidation process on nanoporous aluminum oxide layers properties

In the present chapter of the thesis the influence of imposed electrochemical parameters in anodic oxidation process on nanoporous aluminum oxide layers morphological, compositional and structural characteristics formed by controlled anodic oxidation on 1050 aluminum alloy surfaces were analyzed.

Also, the influence of imposed parameters into anodic oxidation process on the obtained nanoporous aluminum oxide layers thickness was analyzed. The research aimed to determine the nanoporous aluminum oxide layers roughness and wetting properties.

The 1050 aluminum alloy were anodized using potential values between 10 V and 25 V, for different time periods (between 10 minutes to 60 minutes) and different stirring rates of electrolyte.

## 3.1. Morphological characterization using by electron microscopy

The morphological characterization of electrochemical polished 1050 aluminum alloy surfaces before and after the anodic oxidation process was performed using the scanning electron microscope.

### 3.1.1. Evaluation of nanopores diameters formed on aluminum oxide layers obtained by anodic oxidation

The 1050 aluminum oxide samples were electrochemical polished in 15% $Na_2CO_3$ and 5% $Na_3PO_4$ were anodized in 1 M $H_2SO_4$ in which was added 1 g/L $Al_2(SO_4)_3$ x 18 $H_2O$ in order to grow nanoporous aluminum oxide layers on their active surfaces. The applied parameters in the anodic oxidation processes were varied in order to obtain homogeneous aluminum oxide layers. Thereby, the applied potential was varied between 1 V and 24 V, the duration of anodic oxidation process it was ranged between 10 minutes and 480 minutes and the electrolyte stirring rate was ranged between 0 and 700 rpm.

The nanoporous aluminum oxide layers were obtained when the imposed potential was ranged between 15 V and 21 V, the anodic oxidation process duration varied between 25 minutes and 45 minutes and the electrolyte stirring rate was ranged between 0 and 500 rpm.

The surfaces of nanoporous aluminum oxide obtained at 500 rpm electrolyte stirring rate for 45 minutes and the potential ranged between 15 V and 21 V during the anodic oxidation process show nanopores with different widths as could be observed in figure 3.2.

The SEM micrographs taken on the surfaces of nanoporous aluminum oxide layers obtained at 500 rpm electrolyte stirring rate present on an increased number of defects and a decreased porosity. The surface of nanoporous aluminum oxide layer obtained at 15 V present a decreased porosity and a random nanopores distribution, with diameters between 25 nm and 47.6 nm. Applying 18 V and 21 V, respectively, in the anodic oxidation process the aluminum oxide layers porosity increase due to the increasing of nanopores density and decreasing of their diameters. The aluminum oxide layer obtained at 18 V present nanopores with diameters between 17.8 nm and 38 nm and the nanopores widths formed at 21 V are between 25 nm and 30.9 nm.

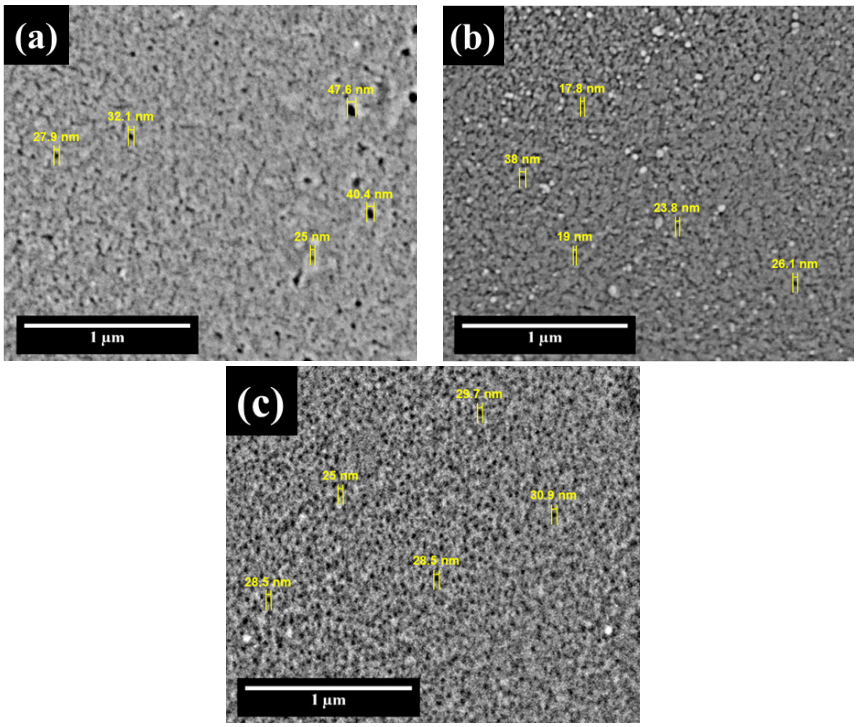


**Figure 3.2.** Evaluation of nanopores diameters from SEM micrographs recorded for anodized surfaces at (a) 15 V, (b) 18 V and (c) 21 V for 45 minutes and 500 rpm stirring rate.

From the SEM micrographs of nanoporous aluminum oxide layers obtained at 0 rpm and 500 rpm stirring rate it could be observed that the aluminum oxide layers porosity and nanopores uniformity simultaneously increase with the increasing of applied potential. Also, the nanoporous aluminum oxide layers obtained at 0 rpm electrolyte stirring rate show an increased porosity and increased nanopores duration in comparison the nanoporous aluminum oxide layers obtained at 500 rpm electrolyte stirring rate.

The influence of anodic oxidation process duration on nanopores diameters formed on the surfaces of aluminum oxide layers obtained at 500 rpm electrolyte stirring rate is presented in figure 3.4.

The SEM micrographs exposed in figure 3.4 show the increasing of aluminum oxide layers porosity and the formed nanopores ordering simultaneously with the increasing of aluminum oxide duration. The increasing of anodic oxidation process duration from 25 minutes to 35 minutes and 45 minutes, has determined the fabrication of aluminum oxide layers with nanopores between 17.2 nm and 25 nm, between 22.6 nm and 32.1 nm and between 25 nm and 30.9 nm, respectively.

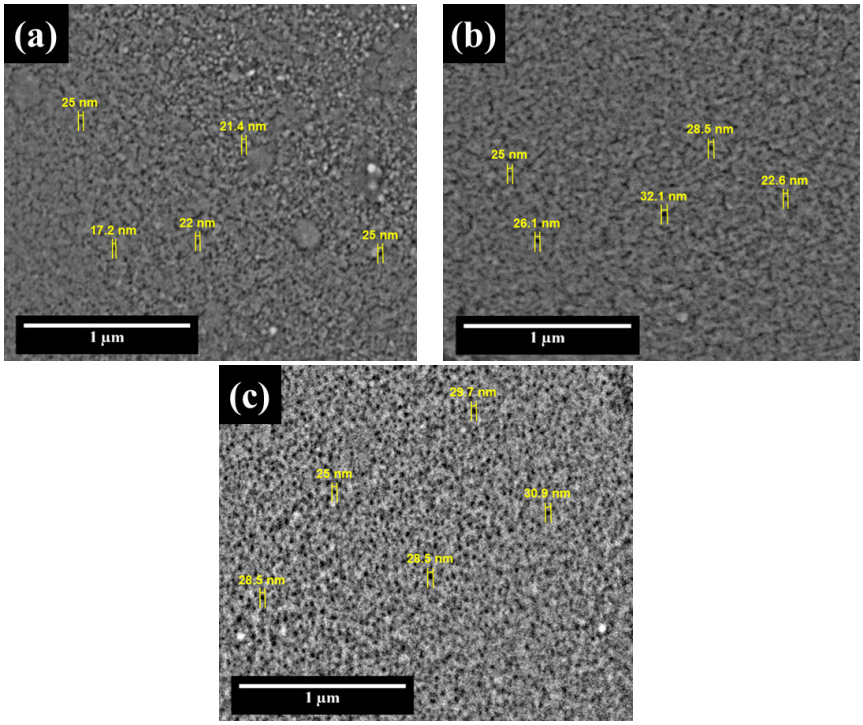


**Figure 3.4.** Evaluation of nanopores diameters from SEM micrographs recorded for anodized surfaces at 21 V for (a) 25 minutes, (b) 35 minutes and (c) 45 minutes and 500 rpm stirring rate.

From the SEM micrographs recorded on the surfaces of nanoporous aluminum oxide layers obtained at 0 rpm and 500 rpm electrolyte stirring rate, it could be observe the increasing of aluminum oxide layers porosity simultaneously with the increasing of anodic oxidation process duration. Also, despite the electrolyte stirring rate, the nanoporous aluminum oxide layers concomitant with the increasing of aluminum oxidation process duration show a nanopores self-ordering tendency.

## 3.1.1. Morphological characterization of electropolished 1050 aluminum alloy

The electrochemical polishing process or electropolishing process of 1050 aluminum alloy samples were done in a solution of 15% $Na_2CO_3$ and 5% $Na_3PO_4$ (known as „Brytal" solution) [3.1, 3.2] in order to clean the Al1050 surface and to decrease the sample's roughness and the number of macroscopic defects.

From figure 3.5 (b) it could be seen that the 1050 aluminum alloy surfaces became smoother after the electrochemical polishing process and also conferred a decreased number of macroscopic defects in comparison with the mechanical polished 1050 aluminum alloy sample presented in figure 3.5 (a).

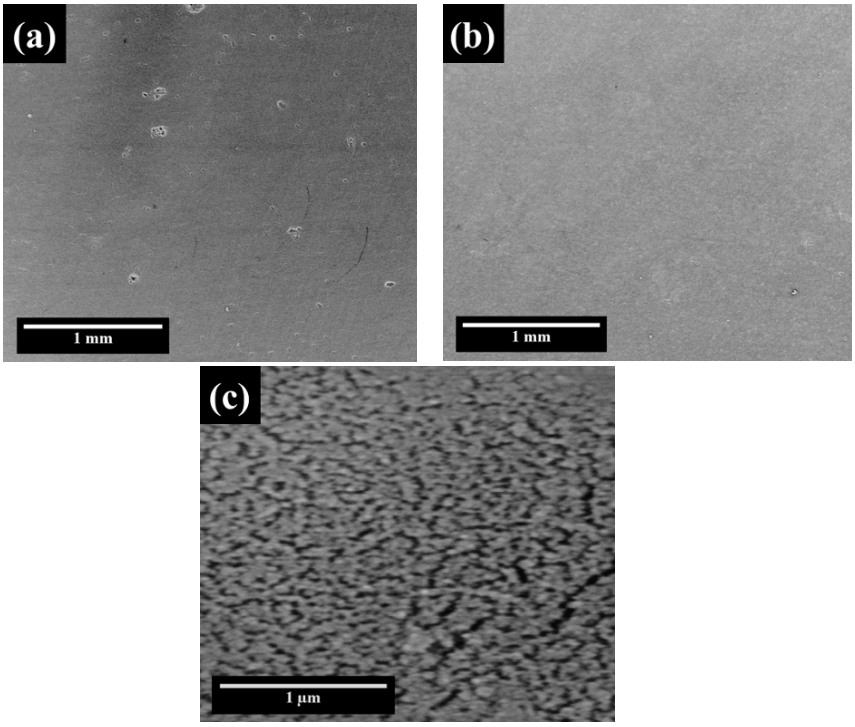


**Figure 3.5.** SEM micrographs of 1050 aluminum alloy surface (a) before and (b) after the electrochemical polishing process, (c) after the electropolishing process at higher magnification

In figure 3.5 (c), at a higher magnification, it is presented the 1050 aluminum alloy surface morphology after the electrochemical polishing process in „Brytal" solution. It is observed that the native aluminum oxide layers that cover the 1050 aluminum alloy surface is not uniform and exhibits crevices with a random distribution and dimensions [3.5].

## 3.1.2. Influence of imposed potential in anodic oxidation process on nanoporous aluminum oxide layers morphology

The SEM micrographs of anodized 1050 aluminum alloy surfaces for 45 minutes at different potential values (15 V, 18 V and 21 V) using an electrolyte stirring rate of 500 rpm are presented in figure 3.7.

From figure 3.7 (a) it could be observed an increase in total defects number and the porosity decrease on the nanoporous aluminum oxide layer surface obtained at 500 rpm electrolyte stirring rate and in imposed potential value of 15 V, and the nanopores diameters are irregular with a random distribution, also.

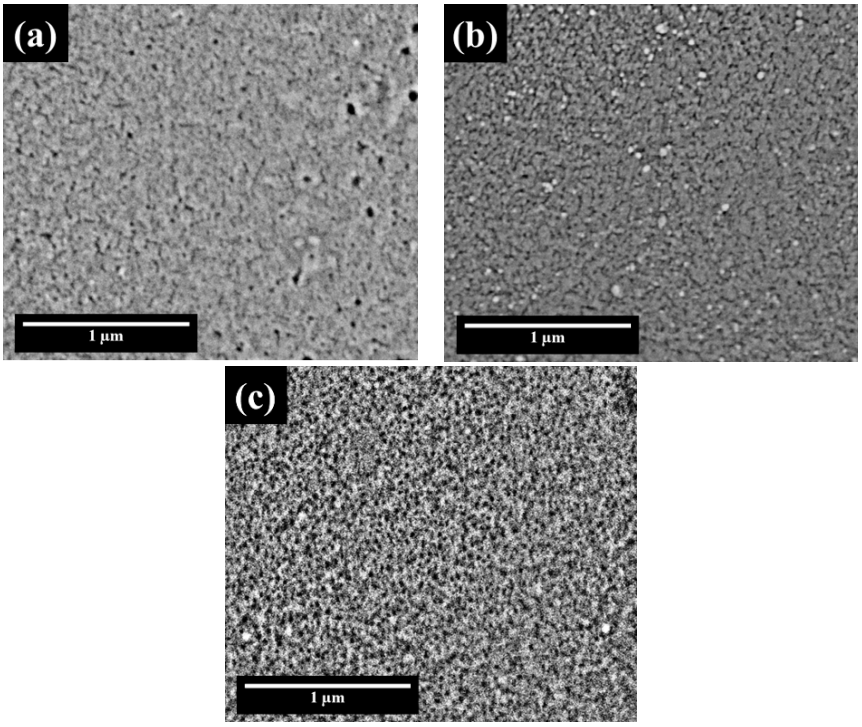


**Figure 3.7.** SEM micrographs of anodized surfaces at (a) 15 V, (b) 18 V and (c) 21 V for 45 minutes at 500 rpm electrolyte stirring rate

The increasing of imposed potential in anodic oxidation process from 15 V to 18 V lead to the decreasing of defects number, the nanopores number increase, but their diameters and distribution are irregular. Increasing the potential value up to 21 V produce an increased porosity of nanoporous aluminum oxide layer and the nanopores distribution is more regular. Also, the defects number decrease in comparison with the nanoporous aluminum oxide layer obtained at 18 V.

The SEM micrographs recorded on nanoporous aluminum oxide layers obtained by anodic oxidation in static conditions of electrolyte revealed an increased porosity and a decreased defects number in comparison with the SEM micrographs of nanoporous aluminum oxide layers anodized at 500 rpm electrolyte stirring rate.

### 3.1.3. Influence of anodic oxidation duration on nanoporous aluminum oxide layers morphology

In figure 3.9 the SEM micrographs of anodized 1050 aluminum alloy at room temperature, 500 rpm electrolyte stirring rate and 21 V for 25 minutes, 35 minutes and 45 minutes are presented. From SEM micrographs presented in figure 3.9 it could be seen that the defects number decrease simultaneously with the increasing of anodizing process duration, from 25 minutes (figure 3.9 (a)) to 35 minutes (figure 3.9 (b)) and 45 minutes (figure 3.9 (c)) respectively.

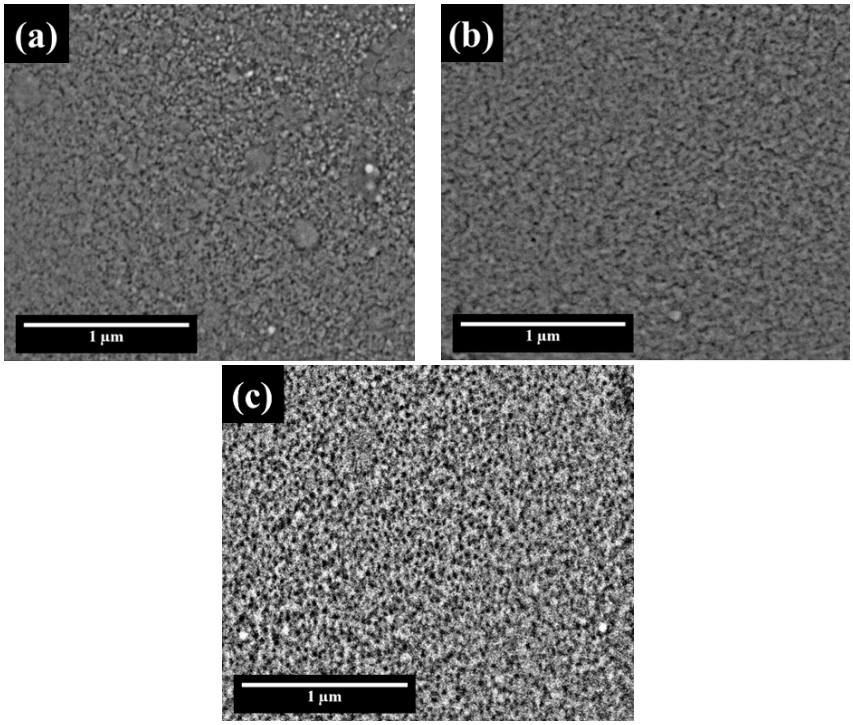


**Figure 3.9.** SEM micrographs of anodized surfaces at 21 V for (a) 25 minutes, (b) 35 minutes and (c) 45 minutes at 500 rpm electrolyte stirring rate

Also, from figure 3.9 it could be observed that the increasing of anodic oxidation process duration using 500 rpm electrolyte stirring rate lead to the increasing of anodized surfaces porosity and the formed nanopores shows a uniform distribution.

The surfaces of obtained nanoporous aluminum oxide layers in static conditions for different durations of anodic oxidation process at 21 V shows an increased porosity and a decreased defects number in comparison with the obtained nanoporous aluminum oxide layers at 500 rpm stirring rate.

The diminishing of defects number and increasing of layer porosity of nanoporous aluminum oxide layers obtained without stirring rate is caused by the rapid dissolution of 1050 aluminum alloy simultaneous with the increasing of electrolyte temperature under the electrical charge during the anodic oxidation process [3.9, 3.11, 3.12].

## 3.2. Evaluation of nanoporous aluminum oxide layer thickness by SEM micrograph in cross section

The nanoporous aluminum oxide layers were analyzed in cross section using the scanning electron microscope to observe the influence of imposed parameters in anodic oxidation process on their thickness. In order to calculate the mean thickness of nanoporous aluminum oxide layers, at least 3 measurements in different spots on each cross section SEM micrographs were made.

### 3.2.1. Influence of imposed potential in anodic oxidation process on nanoporous aluminum oxide thickness

In figure 3.11, the cross-section SEM micrographs of anodized 1050 aluminum alloy samples at room temperature, for 45 minute at 500 rpm electrolyte stirring rate and a potential values between 15 V and 21 V are shown.

From the recorded cross-section SEM micrographs presented in figure 3.11 it could be observed that for the imposed potential value of 15 V during the anodic oxidation process, the obtained nanoporous aluminum oxide layer has 8.46 µm mean thickness.

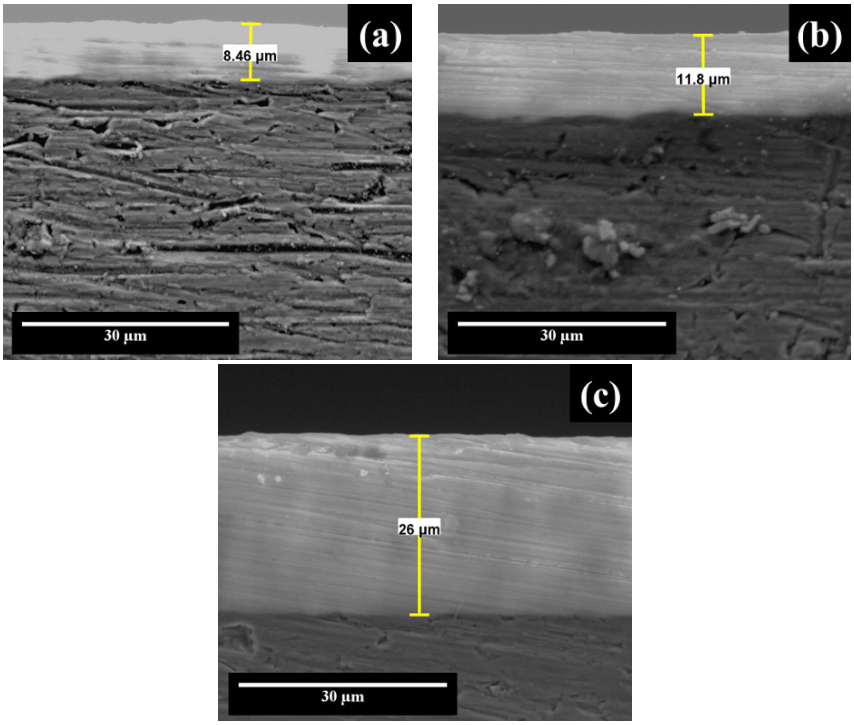


**Figure 3.11.** Cross-section SEM micrographs of anodized surfaces using an imposed potential of (a) 15 V, (b) 18 V and (c) 21 V for 45 minutes in 500 rpm stirring rate

The increasing of imposed potential value from 15 V to 18 V and 21 V during the anodic oxidation process produces the increasing of nanoporous aluminum oxide layers thickness up to 11.8 µm and 26 µm.

In comparison with the thickness of nanoporous aluminum oxide layers obtained at 500 rpm electrolyte stirring rate, the thickness of nanoporous aluminum oxide layers obtained without stirring rate shown increased values due to the increased electrolyte temperature during the anodic oxidation process. Also, the same trend of increasing the nanoporous aluminum oxide layer thickness with the increase of imposed potential during the anodic oxidation process is maintained.

The increasing of nanoporous aluminum oxide layers thickness during the anodic oxidation process was observed by G.D. Sulka and W.J. Sepniwki [3.9] for the aluminum

oxide layers formed on pure aluminum surfaces in 0.3 M oxalic acid and a potential ranged between 30 V and 65 V.

### 3.2.2. Influence of anodic oxidation process duration on nanoporous aluminum oxide thickness

The cross-section SEM micrographs recorded for the 1050 aluminum alloy samples anodized at 500 rpm electrolyte stirring rate and 21 V for 25 minutes, 35 minutes and 45 minutes are presented in figure 3.13.

From figure 3.13 it could be observed that the nanoporous aluminum oxide layers present an increasing thickness trend simultaneous with the increasing of anodic oxidation process duration. The increasing of anodic oxidation process duration from 25 minutes (figure 3.13 (a)) to 35 minute (figure 3.13 (b)) and 45 minutes (figure 3.13 (c)) produce the increasing of nanoporous aluminum oxide layer thickness from 14.2 µm to 23.3 µm to 26 µm

The same increasing trend of nanoporous aluminum oxide layer thickness with the increasing of anodic oxidation process duration was observed by Veys-Renaux et al [3.14] for the nanoporous aluminum oxide layers grown on Al1050 in 2 M sulphuric acid electrolyte, by G.D. Sulka şi W.J. Stepnowski [3.9] for pure aluminum anodized in 0.3 M oxalic acid. R.K. Choudhary and his co-workers [3.12] observe that the increasing of anodizing process duration with 20 minutes lead to 69% increasing of aluminum oxide layer thickness obtained on pure aluminum in 10% oxalic acid.

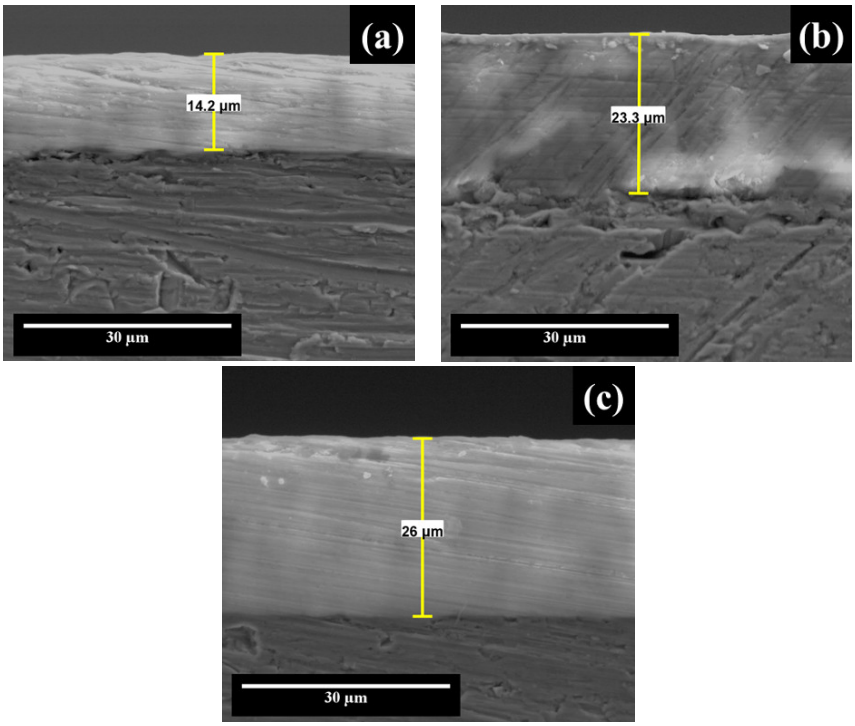


**Figure 3.13.** Cross-section SEM micrographs of anodized surfaces at 21 V in (a) 25 minutes, (b) 35 minutes and (c) 45 minutes using 500 rpm electrolyte stirring rate

The nanoporous aluminum oxide layers obtained at 500 rpm stirring rate show lower thicknesses in comparison with the nanoporous aluminum oxide layers obtained in static conditions at the same potential values or anodizing duration. The same trend of the increasing nanoporous aluminum oxide layer thickness with the increasing of anodizing duration was maintained.

## 3.3. SEM-EDX compositional analysis

The SEM-EDX analyzes were recorded on the entire surfaces of nanoporous aluminum oxide layers in order to be observed an overview of nanoporous aluminum oxide layer chemical composition.

The recorded SEM-EDX weight percent spectrums of electrochemical polished 1050 aluminum alloy and nanoporous aluminum oxide layers, show an increasing trend for the oxygen element weight percent simultaneous with the increasing of potential, anodizing duration and stirring rate and for aluminum and carbon elements, the weight percents spectrum present a decreasing trend.

## 3.4. X-ray diffraction structural analysis

The structural characterization of nanoporous aluminum oxide layers were made using X-ray diffraction method in order the observe the influence of the parameters imposed in the fabrication process on the structural phase modification of nanoporous aluminum oxide layers obtained by anodic oxidation.

The XRD diffractograms reveal the increasing of aluminum oxide peaks intensities simultaneous with the decreasing of metallic aluminum peaks intensities for the nanoporous aluminum oxide layers in comparison with the electrochemical polished 1050 aluminum alloy.

## 3.5. Roughness characterization

The 2D roughness profiles of nanoporous aluminum oxide layers were obtained using a contact-tip roughness tester that are moved for a known distance on samples surfaces and record the vertical movement evolution of the stylus tip. From the 2D roughness profiles, the mean values of roughness parameters Ra of the analyzed samples were calculated.

The evolution of Ra roughness parameters calculated from 2D roughness profiles of analyzed samples reveal morphological changes on the anodized 1050 aluminum alloy surfaces regardless the electrolyte stirring rate. The increasing of anodizing potential at 15 V and 18 V produce the decreasing of Ra parameter and for the anodized samples at 21 V, the Ra values increase in comparison with the Ra value of electrochemical polished 1050 aluminum alloy surface.

## 3.6. Wetting characterization

In order to calculate the mean values of contact angles between the nanoporous aluminum oxide layer surfaces obtained by anodic oxidation process and the distilled water droplet, at least 9 measurements using the goniometer OCA 15 EC on different area from nanoporous aluminum oxide layers surfaces were made.

### 3.6.1. Influence of imposed potential in anodic oxidation process on nanoporous aluminum oxide wetting properties

The mean values of contact angles of nanoporous aluminum oxide layers surfaces obtained in 500 rpm stirring rate for 45 minutes at different potential values are shown in figure 3.33 (b). From figure 3.33 (b) it could be observed that the mean value of contact angle between distilled water droplet and nanoporous aluminum oxide layers decrease simultaneous with the increasing of anodizing potential. For the nanoporous aluminum oxide layer surface obtained at 15 V it was calculated a mean value of 93.53°. The increase of imposed potential value at 18 V and 21 V during the anodic oxidation process cause a decrease of contact angle means value to 92.11° and 90.51° respectively. The decreasing of contact angles means values calculated for the nanoporous aluminum oxide layers is caused by their morphological structure, their porosity and defects number as could be observed from SEM micrographs presented in figure 3.7.

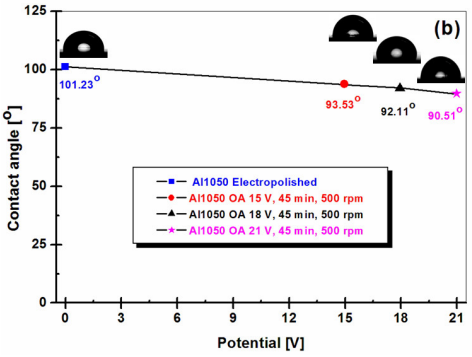


**Figure 3.33.** Influence of imposed potential during the anodic oxidation process on contact angles mean values of nanoporous aluminum oxide layers obtained (b) using 500 rpm electrolyte stirring rate

The nanoporous aluminum oxide layers obtained without stirring rate present decreased means values of contact angles due to their increased porosity in comparison with the nanoporous aluminum oxide layers obtained at 500 rpm electrolyte stirring rate. Also, the same decreasing trend of contact angles mean values with the increasing of potential values imposed in anodic oxidation process is maintained.

### 3.6.2. Influence of anodic oxidation process duration on nanoporous aluminum oxide wetting properties

The mean values of contact angles calculated for anodized 1050 aluminum alloy samples at 500 rpm stirring rate and 21 V for different anodic oxidation duration are presented in figure 3.35 (b).

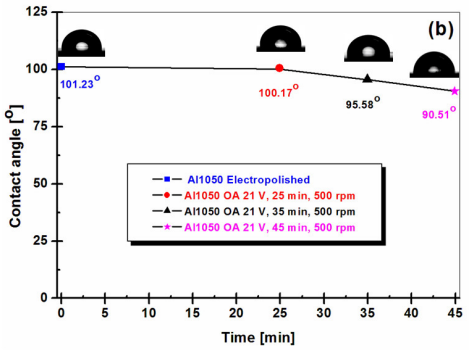


**Figure 3.35.** Influence of anodic oxidation process duration on contact angles mean values of nanoporous aluminum oxide layers obtained (b) using 500 rpm electrolyte stirring rate

From figure 3.35 it could be observed that the contact angle mean values present a decreasing trend with the increasing of anodic oxidation process duration. For the anodized 1050 aluminum alloy sample at 21 V for 25 minute it was calculated a contact angle mean value of 100.17$^{o}$ and the increasing of anodic oxidation process duration up to 35 minutes and 45 minutes cause a decrease of contact angle mean values to 95.58$^{o}$ and 90.51$^{o}$ respectively. The decreasing of contact angles mean values is caused by the nanoporous aluminum oxide layer morphological structure and porosity.

The contact angle mean values of nanoporous aluminum oxide layers obtained without electrolyte stirring rate have the same decreasing trend of contact angle mean values with the increasing of anodic oxidation duration. Also, it could be observed that the increasing of nanoporous aluminum oxide layers obtained without electrolyte stirring rate porosity cause the decrease of contact angles mean values.

## 3.7. Partial conclusions

The anodic oxidation process form on 1050 aluminum alloy surfaces nanoporous aluminum oxide layers that change the surfaces morphology in comparison with the electrochemical polished 1050 aluminum alloy surface.

In the present thesis it was evaluated the influence of imposed parameters in anodic oxidation process on morphological, structural and compositional characteristics of nanoporous aluminum oxide layers. The influences of imposed potential, the influence anodic oxidation process duration and the influence of electrolyte stirring rate on nanoporous

aluminum oxide layers characteristics obtained by controlled anodic oxidation in 1 M $H_2SO_4$ in which was added 1 g/L $Al_2(SO_4)_3$ x 18 $H_2O$ were evaluated.

From top-view SEM micrographs of nanoporous aluminum oxide layers it was observed that the increasing of imposed potential and anodic oxidation process duration lead to the obtaining of a more uniform layers (a reduced defects number) with an increased porosity for nanoporous aluminum oxide layers without electrolyte stirring rate and the obtaining of a more uniform layers with a decreased porosity for nanoporous aluminum oxide layers anodized at 500 rpm electrolyte stirring rate.

The increasing of potential value and anodic oxidation process duration cause an increase of nanoporous aluminum oxide layer thickness, regardless of electrolyte stirring rate.

From contact angles mean values analysis of nanoporous aluminum oxide layers it could be observed a decreasing trend in comparison with the contact angle mean value of electrochemical polished 1050 aluminum alloy. The obtained nanoporous aluminum oxide layers at 15 V and 18 V present an increasing trend despite the electrolyte stirring rate and anodic oxidation process duration and the nanoporous aluminum oxide layers obtained at 21 V despite the electrolyte stirring rate, the contact angle means values show a decreasing trend with the increasing of anodic oxidation process duration.

## 3.8. Selective references of chapter 3

[3.1] A. Rauf, M. Mehmood, M.A. Rasheed, M. Aslam, The effects of electropolishing on the nnaochannel ordering of the porous anodic alumina prepared in oxalic acid, Journal of Solid State Electrochemistry, 13, (2009), 321 – 332, DOI: 10.1007/s10008-008-0550-2

[3.2] G. Schimo, A.W. Hassel, 3D printed double flow cell for local through-thickness anodization in aluminum, Electrochemistry Communications, 69, (2016), 84 – 88, DOI: 10.1016/j.elecom.2016.06.005

[3.5] **V. Dumitrascu**, L. Benea, E. Danaila, Characterization of nanoporous aluminum oxide layers obtained by controlled anodic oxidation, Proceeding Conference of 17th International Multidisciplinary Scientific Geoconference, SGEM 2017, Vol. 17, Micro and Nano Technologies, (2017), 43 – 50, ISBN 978-619-7408-12-6/ISSN: 1314-2704, DOI: 10.5593/sgem2017/61/S24.006

[3.9] G.D. Sulka, W.J. Stepniowski, Structural features of self-organized nanopores arrays formed by anodization of aluminum in oxalic acid at relatively high temperatures, Electrochimica Acta, 54, (2009), 3683 – 3691, DOI: 10.1016/j.electacta.2009.01.046

[3.11] G.D. Sulka, K.G. Parkola, Temperature influence on well-ordered nanopores structures grown by anodization of aluminum in sulphuric acid, Electrochimica Acta, 52 (2007), 1880 – 1888, DOI: 10.1016/j.electacta.2006.07.053

[3.12] R.K. Choudhary, P. Mishra, V. Kain, K. Singh, S. Kumar, J.K. Chakravartty, Scratch behavior of aluminum anodized in oxalic acid: Effect of anodizing potential, Surface and Coatings Technology, 283, (2015), 135 – 147, DOI: 10.1016/j.surfcoat.2015.10.042

[3.14] D. Veys-Renaux, N. Chahboun, E. Rocca, Anodizing of multiphase aluminium alloys in sulfuric acid: in-situ electrochemical behaviour and oxide properties, Electrochimica Acta, 211, (2016), 1056 – 1065, DOI: 10.1016/j.electacta.2016.06.131

# CHAPTER 4.

# The influence of electrochemical parameters imposed in anodic oxidation process on anticorrosive properties of nanoporous aluminum oxide layers

The corrosion resistances of nanoporous aluminum oxide layers obtained by anodic oxidation were determined in 3.5% NaCl solution with a pH value of 5.75, using electrochemical methods and compared with the corrosion resistance of electropolished 1050 aluminum alloy.

Also, in chapter 5, the influence of imposed parameters in anodic oxidation process on the anticorrosive properties of nanoporous aluminum oxide layers was evaluated.

## 4.1. Open circuit potential – OCP

The free potential or open circuit potential is an electrochemical method that offers information about the corrosion behavior of an immersed material into corrosive solution, revealing the interaction tendency between the material and the corrosive environment.

The open circuit potential it was the started method after the samples immersion into corrosive environment in order to observe the interaction between nanoporous aluminum oxide layers with the corrosive solution (3.5% NaCl, pH = 5.75). The open circuit potentials were recorded for 17 hours after immersion in order to be attained a steady state value.

### 4.1.1. Influence of imposed potential in anodic oxidation process on open circuit potential evolution

The influence of imposed potential in anodic oxidation process on open circuit potential evolution recorded for the nanoporous aluminum oxide layers obtained at 45 minutes and 500 rpm electrolyte stirring rate, immersed in 3.5% NaCl solution, is presented in figure 4.1 (b).

For the electrochemical polished 1050 aluminum alloy sample subjected to corrosion assays it was observed that the open circuit potential reaches a steady state value around -700 mV vs. Ag/AgCl, KCl saturated, due to the penetration of native aluminum oxide layer by the chloride ions and the modification of electrolyte pH value near the 1050 aluminum alloy surface [4.1].

From the open circuit potentials diagrams for the nanoporous aluminum oxide layers immersed in 3.5% NaCl solution, it was observed that the free potential reaches the steady

state values after 300 minutes of immersion, regardless of the imposed potential value in anodic oxidation process. The free potential reaches the steady state after 300 minutes due to the nanoporous aluminum oxide layer penetration by the corrosive electrolyte that cause heterogeneous reactions in the presence of chloride ions and due to the heterogeneous morphological, structural and compositional characteristics of the inner barrier-type aluminum oxide film from the bottom of the nanopores. The open circuit potential reaches the steady state values after 300 minutes of immersion due to the passive aluminum oxide layer development that protect the aluminum substrate against aggressive chloride ions from the electrolyte.

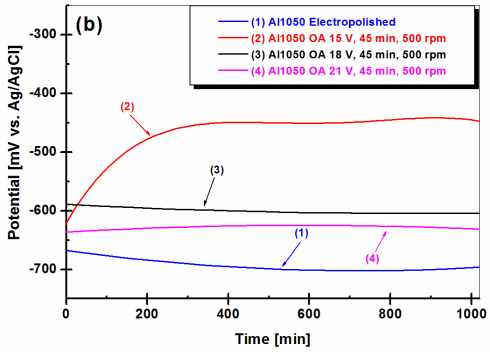


**Figure 4.1.** Evolution of open circuit potential (OCP) for (1) electrochemical polished 1050 aluminum alloy and for the anodized samples at (2) 15 V, (3) 18 V and (4) 21 V for 45 minutes (b) at 500 rpm electrolyte stirring rate, immersed in 3.5% NaCl solution with a pH value of 5.75

From figure 4.1 (b) it can be observed that the open circuit potential recorded for the nanoporous aluminum oxide layers obtained at 500 rpm electrolyte stirring rate is more noble with the decreasing of imposed potential in the anodic oxidation process. For the nanoporous aluminum oxide layer obtained at 15 V, the free potential reaches the steady state at -450 mV vs. Ag/AgCl with an increasing trend in time. By increasing the imposed potential value in anodic oxidation process to 18 V and 21 V, after the immersion of nanoporous aluminum oxide layers in NaCl 3.5%, the free potential reaches the steady state values at -605 mV vs. Ag/AgCl and -630 mV vs. Ag/AgCl, respectively. The decreasing of the free potential steady state could be caused by the increasing of nanopores density simultaneously with the increasing of imposed potential in anodic oxidation process that facilitate the electrolyte penetration including the aggressive chloride ions to the inner barrier-type aluminum oxide film from the bottom of the nanopores.

From figure 4.1. it could be seen that the nanoporous aluminum oxide layers formed by anodic oxidation process attained more noble free potential steady state value in comparison with the free potential steady state value recorded for the electropolished 1050 aluminum alloy. Also, a decreasing trend of free potential is maintained for the nanoporous aluminum oxide layers obtained in static and dynamic electrolyte conditions with the increasing of anodic potential value imposed in the electrochemical process.

### 4.1.2. Influence of anodic oxidation process duration on open circuit potential evolution

In figure 4.2 (b) the open circuit potential diagrams recorded after the immersion in NaCl 3.5% for 17 hours of 1050 aluminum alloy samples anodized at 21 V and 500 rpm stirring rate for 25 minutes, 35 minutes and 45 minutes, respectively, are shown.

For the nanoporous aluminum oxide layer obtained at anodic oxidation duration of 25 minutes, the free potential reaches a steady state around -460 mV vs. Ag/AgCl with a decreasing trend in time. The increasing of anodic oxidation duration from 25 minutes to 35 minutes and 45 minutes cause a decreasing of free potential steady state to -544 mV vs. Ag/AgCl and -630 mV vs. Ag/AgCl, respectively. The free potential steady state is decreasing simultaneously with the increasing of anodic oxidation process duration, caused by the increasing of nanopores density and their diameters also, that allow a facile electrolyte penetration to the inner barrier-type aluminum oxide film from the bottom of nanopores.

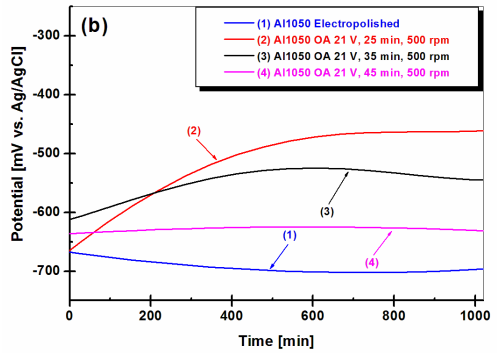


**Figure 4.2.** Evolution in time of open circuit potential for (1) electrochemical polished 1050 aluminum alloy and for the anodized samples at (2) 25 minutes, (3) 35 minutes and (4) 45 minutes for 21 V at (b) 500 rpm electrolyte stirring rate, immersed in 3.5% NaCl solution with a pH value of 5.75

The nanoporous aluminum oxide layers formed at 0 rpm stirring rate maintain the same decreasing trend of the free potential steady state with the increasing of anodic oxidation process duration. Even if, the nanoporous aluminum oxide layers obtained at 0 rpm stirring rate show a decreasing trend for free potential steady state, the steady state values are more noble in comparison with the free potential steady state recorded for the electropolished 1050 aluminum alloy sample.

## 4.2. Electrochemical impedance spectroscopy - EIS

The electrochemical impedance spectroscopy is an electrochemical method in A. C. used to characterize the electrode-electrolyte interface processes.

In the corrosion assays, the EIS diagrams show complete information about processes kinetics that take place at the electrode-electrolyte (corrosive solution) interface [4.11, 4.12].

The Nyquist representation of EIS diagrams is used in literature because it allows an easy identification of equivalent circuit elements that are used to fit the recorded experimental data and to calculate the values of the polarization resistances.

Due to the analyzed surface porosity and/or inhomogeneity [4.13, 4.14], the EIS diagrams were fitted with simple and complex elements such as resistors and constant phase elements (CPE). The constant phase element allows the representation of dispersed frequency and their value is calculated using A. Lasia relation [4.15]:

$$Z_{CPE} = \frac{1}{Q(j\omega)^{\alpha}} \qquad (4.1)$$

where: $j = \sqrt{-1}$, ω is angular frequency (ω=2πf, f is frequency in Hz), Q is a real constant (F $cm^{-2}$ $s^{(1-\alpha)}$) and α is related by the angular rotation of a purely capacitor element on the complex plane.

In order to fit the EIS diagram recorded for the electrochemical polished 1050 aluminum alloy immersed in NaCl 3.5%, it was used a simple electrical circuit, exposed in figure 4.3. In figure 4.3, $R_s$ is the electrolyte resistance, $R_e$ and $CPE_e$ are the polarization resistance and constant phase element of the electrochemical polished surface, respectively.

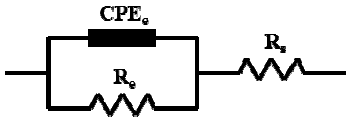


**Figure 4.3**. Equivalent circuit used to fit the EIS diagrams recorded for the electropolished Al1050 and expose to corrosion assays in 3.5% NaCl with a pH = 5.75

In figure 4.4 it is presented the equivalent circuit used to fit the EIS diagrams recorded for the nanoporous aluminum oxide layers obtained at different electrochemical parameters. The nanoporous aluminum oxide layer could be divided in two parts (a part is the aluminum oxide outer layer formed by the nanoporous structure and a part is the barrier-type inner layer from the bottom of nanopores), so it was used a simple equivalent circuit for each part and after that the equivalent circuits were connected in series.

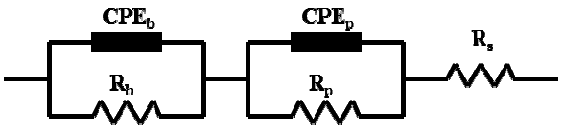


**Figure 4.4**. Equivalent circuit used to fit the EIS diagrams recorded for the nanoporous aluminum oxide layers exposed to corrosion assays in 3.5% NaCl with a pH = 5.75.

From figure 4.4 it could be seen that the Rs is the solution resistance, Rp and CPEp are the polarization resistance and the constant phase element of outer nanoporous aluminum oxide layer and $R_b$ and $CPE_b$ are the polarization resistance and the constant phase element of the inner barrier-type aluminum oxide layer from the bottom of the nanopores, respectively.

The polarization resistance of the analyzed samples could be determined at the intersection between the impedance semicircle and the abscissa or by fitting the experimental data using an equivalent circuit.

The electrochemical impedance spectroscopy was carried out after 17 hours of samples immersion into electrolyte, time period in which in the electrochemical cell was attained the potential steady state, the frequency was ranged between $10^5$ Hz and $10^1$ Hz using a small amplitude A.C. signal of 10 mV, being recorded 10 points per decade. The EIS diagrams were fitted with Zview 3.4f software and the quality of the fitted results were evaluated using the chi-square ($chi^2$) element with a value bellow $10^{-3}$.

### 4.2.1. Influence of imposed potential in anodic oxidation process on polarization resistance evolution from electrochemical impedance spectroscopy diagrams

In figure 4.6 (a) are shown, in Nyquist representation, the EIS diagrams of the electropolished 1050 aluminum alloy and the nanoporous aluminum oxide layers obtained at 500 rpm electrolyte stirring rate for 45 minute and the potential were ranged between 15 V and 21 V. In figure 4.6 (b) a zoom of the EIS diagrams in the high frequency domain is presented, in order to obtain a better view of the electropolished 1050 aluminum alloy EIS diagram. The EIS recorded experimental data were represented using symbols and the fitted EIS results using the equivalent circuits from figure 4.3 and figure 4.4 are represented with a continuous line.

The EIS diagram recorded for the electropolished 1050 aluminum alloy present a capacitive loop with a reduced height in comparison with the EIS diagrams recorded for the nanoporous aluminum oxide layers that indicate a decreased corrosion resistance in comparison with the corrosion resistance of the nanoporous aluminum oxide layers. The EIS diagram of electropolished 1050 aluminum alloy was fitted with the equivalent circuit presented in figure 4.3 and the values of circuit elements are exposed in the table 4.1. For the electropolished 1050 aluminum alloy it was determined a polarization resistance value around *25.781 kohm cm$^2$*.

***Table 4.1.*** *The elements values of equivalent circuit used to fit the experimental date recorded for the electropolished 1050 aluminum alloy*

| **Equivalent circuit elements** | **Electropolished Al1050 surface** |
|---|---|
| **$R_s$** [$\Omega$ cm$^2$] | 10.9 |
| **$CPE_e$** [F cm$^2$ s$^{(1-\alpha)}$] | 5.2975 E$^{-6}$ |
| **$\alpha_e$** | 0.88556 |
| **$R_e$** [$\Omega$ cm$^2$] | 25781 |
| **Chi$^2$** | 0.8113 E$^{-3}$ |

From figure 4.6 it can be seen that the EIS diagrams recorded for the nanoporous

aluminum oxide layers show the same capacitive loop. The imposed potential increase in the anodic oxidation process induces the increasing of the capacitive loops heights-meaning that the corrosion resistance is increasing.

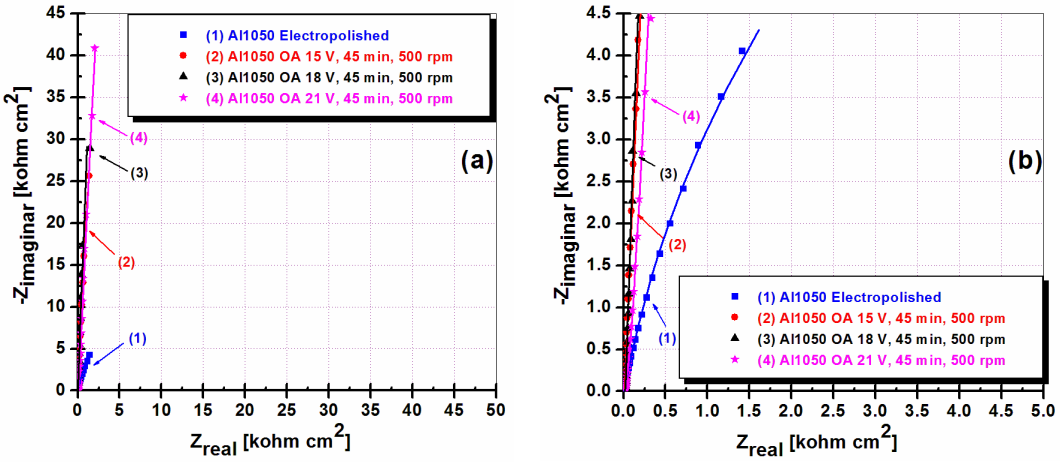


**Figure 4.6.** (a) The Nyquist representation of EIS diagrams recorded for (1) electropolished surface and anodized surfaces at (2) 15 V, (3) 18 V and (4) 21 V for 45 minutes at 500 rpm electrolyte stirring rate, immersed in 3.5% NaCl solution with a pH = 5.75 and (b) zoom of Nyquist diagrams in order to obtain a better view of EIS diagram recorded for the electropolished surface.

The EIS diagrams recorded for the nanoporous aluminum oxide layers were fitted using the equivalent circuit from figure 4.4 and in table 4.3 the values of equivalent circuit elements are presented.

From table 4.3 it could be seen that the increasing of the imposed potential in the anodic oxidation process from 15 V to 18 V causes the increasing of polarization resistance from *2596.9 kohm cm²* to *4105.8 kohm cm²* and the increasing of anodizing potential up to 21 V increase the polarization resistance to *36850 kohm cm²*.

***Table 4.3.*** *The elements values of equivalent circuit used to fit the experimental date recorded for the nanoporous aluminum oxide layers obtained at 45 minutes and 500 rpm electrolyte stirring rate*

| **Equivalent circuit elements** | **Potential imposed in anodic oxidation process** [V] | | |
|---|---|---|---|
| | **15** | **18** | **21** |
| $\mathbf{R_s}$ [Ω cm²] | 14.3 | 15.4 | 16.1 |
| $\mathbf{CPE_p}$ [F cm² s$^{(1-\alpha)}$] | 1.1129 E$^{-3}$ | 6.0594 E$^{-5}$ | 7.2014 E$^{-5}$ |
| $\boldsymbol{\alpha_p}$ | 0.625 | 0.634 | 0.623 |
| $\mathbf{R_p}$ [Ω cm²] | 33.2 | 43.67 | 95.57 |
| $\mathbf{CPE_b}$ [F cm² s$^{(1-\alpha)}$] | 5.5161 E$^{-7}$ | 5.4091 E$^{-7}$ | 4.3789 E$^{-7}$ |
| $\boldsymbol{\alpha_b}$ | 0.969 | 0.967 | 0.97 |
| $\mathbf{R_b}$ [Ω cm²] | 2.596.9 E$^{6}$ | 4.105.8 E$^{6}$ | 3.685 E$^{7}$ |
| **Chi²** | 0.7914 E$^{-3}$ | 0.6642 E$^{-3}$ | 0.6007 E$^{-3}$ |

By comparing the EIS diagrams recorded for the nanoporous aluminum oxide layers obtained at 0 rpm and 500 rpm electrolyte stirring rate it could be observed that the diagram maintains the same capacitive loop aspect and their heights increase simultaneously with the increasing of anodizing potential.

The increasing of polarization resistance is influenced by the increasing of nanoporous aluminum oxide layer thickness, in specially, that cause the growth of the barrier-type aluminum oxide layer from the bottom of the nanopores. Also, the decreasing of nanoporous aluminum oxide layer porosity obtained at 500 rpm electrolyte stirring rate in comparison with the porosity of nanoporous aluminum oxide layers obtained at 0 rpm electrolyte stirring rate increase the polarization resistance.

## 4.3. Potentiodynamic polarization – PD

The potentiodynamic polarization diagrams are used to study the kinetics of corrosion processes in order to determine the passive domains of materials after the immersion into corrosive electrolytes. The passive domain means the formation of the oxide layer at the material–electrolyte interface that cause the decreasing of the corrosion current value in the analyzed potential domain. By analyzing the potentiodynamic polarization diagrams it could be identified 4 activity domains at the material–electrolyte interface [4.17]:

- the cathodic domain: the potential domain in which the material surface passive layer is damaged by the hydrogen release;
- the critical domain: is the potential domain where the formation and the dissolution of the passive layer is taking place simultaneously;
- the passive domain, which is the potential domain in which the passive layer is formed;
- the transpassive domain, is the potential domain in which the passive layer breaks down and the substrate is damaged.

By analyzing the potentiodynamic polarization diagrams, the passive domains especially (their length and the current density values), could determine the anticorrosive performances of analyzed materials.

The analyzed surfaces, the electropolished 1050 aluminum alloy and the nanoporous aluminum oxide layers obtained at different electrochemical parameters, were cathodically treated at -2.1 V vs. Ag/AgCl for 3 minutes before the recording the potentiodynamic polarization diagrams in a potential domain ranged between -1.45 V vs. Ag/AgCl and -0.4 V vs. Ag/AgCl with a scanning rate of 1 mV/s.

The analysis of potentiodynamic polarization diagrams show that the increasing of imposed parameters values in the anodic oxidation process cause the increasing of the recorded passive domains lengths and the decreasing of current density recorded in the passive and transpassive domains.

## 4.4. Cyclic voltammetry – CV

The cyclic voltammetry (current density versus potential) is an electrochemical method used to evaluate the nanoporous aluminum oxide layers surface behavior at pitting corrosion. From the linear representation of cyclic voltammograms it could be identified the specific pitting hysteresis after the potential scanning direction is reversed, and the highest hysteresis surface indicate the pitting corrosion susceptibility [4.22, 4.23].

Before the recording of cyclic voltammograms, the analyzed surfaces were cathodically treated at -2.1 V vs. Ag/AgCl for 3 minutes. The cyclic voltammograms were recorded for the electropolished 1050 aluminum alloys and the anodized surfaces at different parameters between -1.45 V vs. Ag/AgCl and -0.4 V vs. Ag/AgCl, the scanning direction was from -1.45 V vs. Ag/AgCl to -0.4 V vs. Ag/AgCl and after reversed to -1.45 V vs. Ag/AgCl, with a scanning rate of 1 mV/s.

By evaluating the cyclic voltammetry diagrams recorded for the anodized surfaces it could be observed that the current density values from the reverse sweep in comparison with direct sweep means the decreasing of hysteresis surfaces simultaneously with the increasing of the imposed potential or anodic oxidation duration. The decreasing of hysteresis surfaces formed by the reversed branch of cyclic voltammograms determine the decreasing of pitting corrosion susceptibility of nanoporous aluminum oxide layers in comparison with the electropolished 1050 aluminum alloy surface.

## 4.5. Partial conclusions

The surfaces of the nanoporous aluminum oxide layers obtained by anodic oxidation in 1 M $H_2SO_4$ in which 1 g/L $Al_2(SO_4)_3$ x 18 $H_2O$ was added and at different electrochemical parameters that were subjected to corrosion assays in 3.5% NaCl solution, pH = 5.75, in order to evaluate the corrosion behavior in comparison with the performances of the electropolished 1050 aluminum alloy surface. Also, the influence of anodizing parameters on the anticorrosive properties of the nanoporous aluminum oxide layers was evaluated.

By analyzing the recorded open circuit potential diagrams for the electropolished 1050 aluminum alloy and the nanoporous aluminum oxide layers it could be observed that the open circuit potential of the nanoporous aluminum oxide layers show noble values and by increasing the potential value or anodic oxidation duration, the open circuit potential steady state decrease for the nanoporous aluminum oxide layers obtained at 0 rpm and 500 rpm electrolyte stirring rate.

The electrochemical impedance spectroscopy method show that all the applied parameters in the anodic oxidation process affects the anticorrosive properties of the nanoporous aluminum oxide layers obtained. By increasing the anodic oxidation process duration and the applied potential, the polarization resistances, determined using equivalent circuits, for the nanoporous aluminum oxide layers presents an increasing trend for both static and dynamic electrolyte conditions. Also, it could be observed that the nanoporous aluminum oxide layers obtained at 500 rpm electrolyte stirring rate show increased values of polarization

resistance in comparison with the nanoporous aluminum oxide layers anodized at 0 rpm electrolyte stirring rate.

After the corrosion assays, it was observed that the anodic oxidation process improves the anticorrosive properties of electropolished 1050 aluminum alloy. Also, by increasing of potential values from 15 V to 21 V and the anodic oxidation process duration from 25 minutes to 45 minutes, the nanoporous aluminum oxide layers obtained show improved anticorrosive properties.

## 4.6. Selective references of chapter 4

[4.1] K. Mansouri, K. Ibrik, N. Bensalah, A. Abdel-Wahab, Anodic dissolution of pure aluminum during electrocoagulation process: Influence of supporting electrolyte, initial pH and current density, Industrial and Engineering Chemistry Research, 50, (2011), 13362 – 13372,
DOI: 10.1021/ie201206d
[4.11] Y. Huang, H. Shih, H. Huang, J. Daugherty, S. Wu, S. Ramanathan, C. Chang, F. Mansfeld, Evaluation of the corrosion resistance of anodized aluminum 6061 using electrochemical impedance spectroscopy (EIS), Corrosion Science, 50, (2008), 3569 – 3575,
DOI: 10,1016/j.corsci.2008.09.008
[4.12] J.A. Gonzalez, V. Lopez, A. Bautista, E. Otero, Characterization of porous aluminium oxide films from a.c. impedance measurements, Journal of Applied Electrochemistry, 29, (1999), 229 – 238, DOI: 10.1023/A:1003481418291
[4.13] **V.M. Dumitrascu**, L. Benea, Improving the corrosion behaviour of 6061 aluminum alloy by controlled anodic formed oxide layer, Revista de Chimie, 68, (2017), 77 – 80, ISSN: 2537-5733, http://www.revistadechimie.ro/article_ro.asp?ID=5393 (accesat în data de 8 ianuarie 2018)
[4.14] J.-B. Jorcin, M.E. Orazem, N. Pebere, B. Tribollet, CPE analysis by local electrochemical impedance spectroscopy, Electrochimica Acta, 51, (2006), 1473 – 1479,
DOI: 10.1016/j.electacta.2005.02.128
[4.15] A. Lasia, Electrochemical impedance spectroscopy and its applications, in Modern aspects of electrochemistry, edited by B.E. Conway, J.O`M. Bockris, R.E. White, Kluwer Academic Publishers, New York, SUA, 2002, 143–248, ISBN: 0-306-46916-2
[4.17] E. Danaila, I. Bounegru, L. Benea, A. Chiriac, Improving biocompatibility of Co-Cr alloy used in dentistry by surface modification with electrochemical methods – corrosion of untreated Co-Cr alloy in solution with different pH, , The Annals of „Dunarea de Jos" University of Galați, Fascicle IX. Metallurgy and Materials Science, No. 2 – 2014, ISSN 1453 – 083X
[4.22] L. Wang, L. Chen, Z. Yan, H. Wang, J. Peng, Effect of potassium fluoride on structure and corrosion resistance of plasma electrolytic oxidation films formed on AZ31 magnesium alloy, Journal of Alloys and Compounds, 480, (2009), 469 – 474,
DOI: 10.1016/j.jallcom.2009.01.012
[4.23] D. Shen, G. Li, C. Guo, J. Zou, J. Cai, D. He, H. Ma, F. Li, Microstructure and corrosion behavior of micro-arc oxidation coating on 6061 aluminum alloy pre-treated by high-temperature oxidation, Applied Surface Science, 287, (2013), 451 – 456, DOI: 10.1016/j.apsusc.2013.09.178

# CHAPTER 5.

# The effect of electrochemical parameters imposed in the anodic oxidation process on wear behavior of aluminum oxide layers

In chapter 5, the influence of electrochemical parameters imposed in the anodic oxidation processes on the wear behavior (mechanical properties) of the nanoporous aluminum oxide layers obtained was evaluated. The wear behavior of electropolished and anodized 1050 aluminum alloy was evaluated using TRM 1000 tribometer (Wazau, Germany) from Research and Development Center for Thermoset Composites Center of „Dunărea de Jos" University of Galați, in a Pin-on-Disc configuration, method that is described in subsection 2.3.6.

In order to evaluate the wear behavior of the nanoporous aluminum oxide layers the friction coefficients diagrams recorded during the wear tests were evaluated, in which a 5 N normal force was applied, in order to simulate force used in industrial domains such as transports (panels for vehicles door), construction (building elements and roofs), advertising (volumetric letters) or equipments production (parts for generators/transformators) where the used materials need to have cumulated properties: low weight, weldability, corrosion resistance and/or wear resistance, etc.. Using ex-situ methods, the wear tracks formed on the nanoporous aluminum oxide layers surfaces were analyzed.

## 5.1. Friction coefficient

The friction coefficient is a dimensionless unit that represents the relation between the modules of two forces that acts vertical (normal force) and parallel (tangential force) at two contact objects interface [5.1, 5.2].

$$\mu = F_t / F_n \tag{5.1}$$

where:
$\mu$= friction coefficient; $F_t$= module of tangential force; $F_n$= module of normal force.

The friction coefficient is an important factor that affects the choosing of the materials to be used in specific environments [5.1].

The friction tests of nanoporous aluminum oxide layers were carried out applying 5 N normal force for 50 minutes and 9.55 rpm sliding speed.

### 5.1.1. The effect of imposed potential in anodic oxidation process on aluminum oxide layers friction coefficients

In figure 5.1 (b) are exposed the friction coefficient diagrams of nanoporous aluminum oxide layers grown at 45 minutes anodic oxidation duration, with a potential ranged between 15 V and 21 V at 500 rpm electrolyte stirring rate.

Friction coefficient diagram recorded for the electropolished 1050 aluminum alloy are shown in figure 5.1 (b) and presents a decreasing trend with the increasing of sliding distance due to the tribolayer formation in the contact area between the analyzed sample and the alumina ball (the pin).

From figure 5.1 (b) it could be observed that the nanoporous aluminum oxide layers present a mean value of friction coefficient decreased in comparison with the mean value of friction coefficient recorded for the electropolished 1050 aluminum alloy, around 0.484. Also, it could be observed that the increasing of imposed potential in the anodic oxidation process cause the decreasing of the recorded friction coefficients mean values, from 0.461 for the nanoporous aluminum oxide layer formed at 15 V to 0.317 and 0.273 for the nanoporous aluminum oxide layers anodized at 18 V and 21 V, respectively.

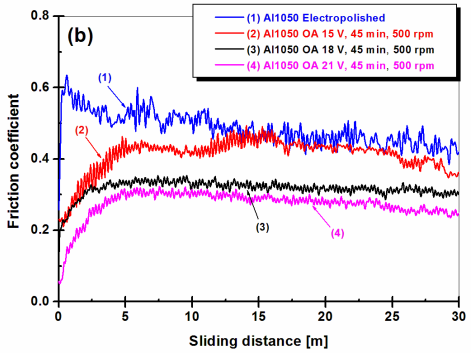


**Figure 5.1.** The influence of imposed potential in the anodic oxidation process on the friction coefficients variation recorded for the nanoporous aluminum oxide formed (b) at 500 rpm electrolyte stirring rate

The friction coefficient diagram recorded for the nanoporous aluminum oxide layer obtained at 15 V present variations in the first 15 meters due to the degradation of nanoporous aluminum oxide layers that have a low thickness (subsection 3.2).

Comparing the friction coefficients diagrams recorded for the nanoporous aluminum oxide layers obtained at 0 rpm and 500 rpm electrolyte stirring rate it could be seen that regardless of imposed electrochemical parameters, the friction coefficients diagrams show a decreasing trend simultaneously with the increasing of sliding distance due to the formation of tribolayers in the contact area between the surfaces and alumina ball. Also, the formed tribolayers act as lubricants, decreasing the friction coefficients [5.7].

The mean values of friction coefficients recorded for the nanoporous aluminum oxide layers anodized at 0 rpm electrolyte stirring rate have increased values in comparison with the mean values of nanoporous aluminum oxide layers obtained at 500 rpm electrolyte stirring

rate due to the increased porosity, except the friction coefficients diagrams recorded for the nanoporous aluminum oxide layers anodized at 15 V. During the friction tests, due to the low thickness, the nanoporous aluminum oxide layer obtained at 15 V and 500 rpm electrolyte stirring rate is damaged leading to value of friction coefficient increase.

W. Bensalah et al [5.8] have observed that the mechanical properties of nanoporous aluminum oxide layers formed on 1050 aluminum alloy increase simultaneously with the decreasing of electrolyte temperature and increasing of imposed current density during the anodic oxidation process, respectively.

The nanoporous aluminum oxide layer obtained at 21 V and 500 rpm electrolyte stirring rate, due to the complex morphological structure and high thickness show the lowest value of the friction coefficient and offer to 1050 aluminum alloy substrate an increased resistance under mechanical factors actions.

## 5.1.2. The effect of anodic oxidation process duration on aluminum oxide layers friction coefficients

The friction coefficient diagrams recorded for the nanoporous aluminum oxide layers anodized at 21 V and 500 rpm electrolyte stirring rate for different time periods are shown in figure 5.3 (b). The friction coefficients diagrams recorded for the nanoporous aluminum oxide layers show lower values in comparison with the friction coefficient mean value of the electropolished 1050 aluminum alloy, around 0.484.

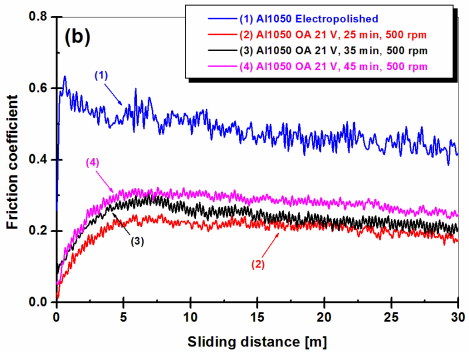


**Figure 5.3.** Influence of the anodic oxidation process duration on the friction coefficients variation recorded for the nanoporous aluminum oxide formed (b) at 500 rpm electrolyte stirring rate

By increasing the anodic oxidation processes duration from 25 minutes to 35 minutes and 45 minutes, respectively, the friction coefficients mean values increase from 0.203 up to 0.235 and 0.273, respectively, due to the increased porosity. The increasing of aluminum oxide layer porosity cause the decreasing of the nanopore walls thickness and also, the decreasing of the wear resistance.

By comparing the friction coefficients diagrams it could be observed that the nanoporous aluminum oxide layers obtained at a decreased anodic oxidation process duration show an increased wear resistance, indifferent by the electrolyte stirring rate. Also, it could be

seen that the decreased porosity of nanoporous aluminum oxide layers formed at 500 rpm electrolyte stirring rate it causes the decreasing of friction coefficients in comparison with the nanoporous aluminum oxide layers anodized at 0 rpm electrolyte stirring rate.

The decreasing of the friction coefficients caused by the porosity increasing was observed by N. Tyntsaru and her coworkers [5.10] for the nanoporous aluminum oxide layers obtained in sulphuric acid on pure aluminum surfaces.

## 5.2. Morphological characterization of wear tracks

The wear tracks morphological characterization was done using the scanning electron microscope FEI Quanta 200 from „Dunărea de Jos" University of Galați. The wear tracks widths were determined in 4 cardinal points and after that their mean values were calculated. In the subsection 5.2, the SEM micrographs where the wear tracks have the width closest to the mean value will be shown.

### 5.2.1. Morphological characterization of wear tracks formed on electropolished 1050 aluminum alloy

In figure 5.5, the wear track formed on the electropolished 1050 aluminum alloy surface subjected to friction tests applying 5 N normal force for 50 minutes and 9.55 rpm sliding speed is presented.

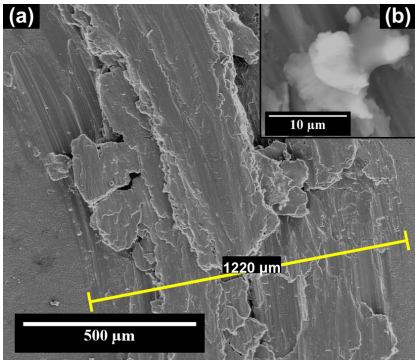


**Figure 5.5.** SEM micrographs of the wear track formed on the electropolished 1050 aluminum alloy (a) entire width of wear track and (b) wear debris formed inside the wear track at a higher resolution

From figure 5.5 (a) it could be observed that wear track width has a mean value of 1220 µm. In the contact area between the alumina ball and the electropolished 1050 aluminum alloy surface can be observed the formation of a discontinuous tribolayer, being visible numerous wear debris, material ruptures and crevices. As can be seen in figure 5.5 (b), the wear debris have different width and forms.

Aluminum and its alloys are liable to adhesive wear due to their increased ductility. The wear debris formed are not removed from the tested surface and during the friction tests

are stacked to the tribolayer formed in the contact area between the alumina ball and the tested sample. P. Groche and F. Resch [5.13], also, have observed that the 1050 aluminum alloy present an adhesive wear during the friction assays.

### 5.2.2. The effect of imposed potential in anodic oxidation process on morphological characterization of wear tracks formed on aluminum oxide layers

In figure 5.7 are exposed the wear tracks formed on the nanoporous aluminum oxide layers surfaces anodized at 500 rpm electrolyte stirring rate for 45 minutes and a potential ranged between 15 V and 21 V.

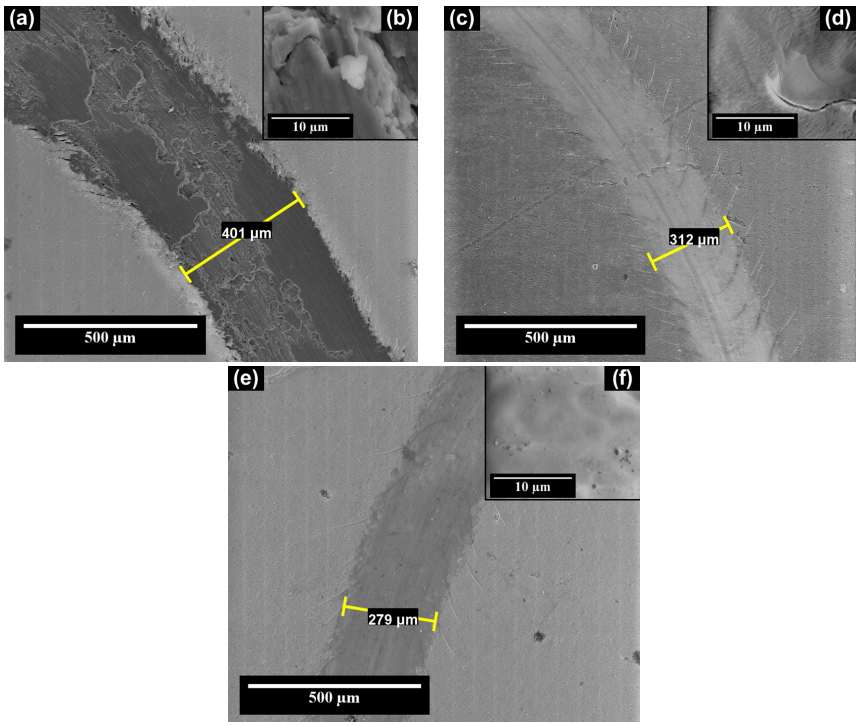


**Figure 5.7.** SEM micrographs of the wear tracks formed on the anodized surfaces at (a) 15 V, (c) 18 V and (e) 21 V for 45 minutes at 500 rpm electrolyte stirring rate. (b), (d) and (f) SEM micrographs taken inside the wear tracks at an increased resolution

The wear tracks formed on the surface of the nanoporous aluminum oxide layer formed at 15 V (figure 5.7 (a and b)) show an increase in defects number, detachments and material ruptures. The wear track width formed on the nanoporous aluminum oxide layer anodized at 15 V has the highest mean value of 401 µm, from the nanoporous aluminum oxide layers obtained at 500 rpm electrolyte stirring rate. At higher resolution (figure 5.7 (b)), inside the wear track, material detachments and wear debris with different sizes and shapes can be identified.

In figure 5.7 (c and d) the wear track formed on the nanoporous aluminum oxide layer

anodized at 18 V with a mean width of 312 μm is presented. On the nanoporous aluminum oxide layer obtained at 18 V it can be observed a few cracks in the outer region of wear track with a small depth. Inside the wear track, at a higher resolution, on the formed tribolayer in the contact area material ruptures are presented.

From figure 5.7 (e and f) it can be seen that the wear track formed on the nanoporous aluminum oxide layer surface, anodized at 21 V has the lowest width with a mean value around 279 μm, and also, a diminished defects frequency at both resolutions. The increased thickness and porosity of the nanoporous aluminum oxide layers obtained at 21 V improve the wear behavior of the 1050 aluminum alloy substrate.

By comparing the wear tracks widths formed on the surfaces of the nanoporous aluminum oxide layers anodized for 45 minutes at 0 and 500 rpm electrolyte stirring rate and a potential ranged between 15 V and 21 V, it could be seen a decreasing trend simultaneously with the increasing of the anodic potential imposed. Also, by increasing of the electrolyte stirring rate from 0 to 500 rpm, the wear tracks width decrease so the wear resistance of the nanoporous aluminum oxide layers increase due to the increasing of nanopores walls.

### 5.2.3. The effect of anodic oxidation process duration on morphological characterization of wear tracks formed on aluminum oxide layers

In figure 5.9, the influence of the anodic oxidation process width on the morphology of wear tracks formed on nanoporous aluminum oxide layers obtained at 21 V and 500 rpm electrolyte stirring rate is presented.

From SEM micrographs shown in figure 5.9, it could be seen that the wear tracks width decrease simultaneously with the increasing of anodic oxidation process duration. The wear tracks formed on the nanoporous aluminum oxide layers anodized for 25 minutes is exposed in figure 5.9 (a) and has a mean width around 320 μm. In the contact area between the surface and the alumina ball an increased numbers of cracks are presented, with different dimensions and depths that starts from the inner to the outer regions of the formed tribolayer. The SEM micrographs exposed in figure 5.9 (b) confirm that the tribolayer formed is not uniform, being visible cracks.

The nanoporous aluminum oxide layers obtained at 35 minutes and 45 minutes have on their surfaces wear tracks with mean values around 286 μm and 279 μm, respectively. In the contact area between alumina ball and analyzed surfaces, the formed tribolayers are uniform on entire surfaces and the defects numbers are insignificant as density or sizes.

Comparing the wear tracks formed on the surfaces of nanoporous aluminum oxide layers during the friction tests it can be seen that the increasing of the anodic oxidation process duration decrease the wear tracks width. Also, it can be observed that the increasing of the electrolyte stirring rate from 0 to 500 rpm during the anodic oxidation process cause morphological changes that increase the wear resistance of the nanoporous aluminum oxide layers.

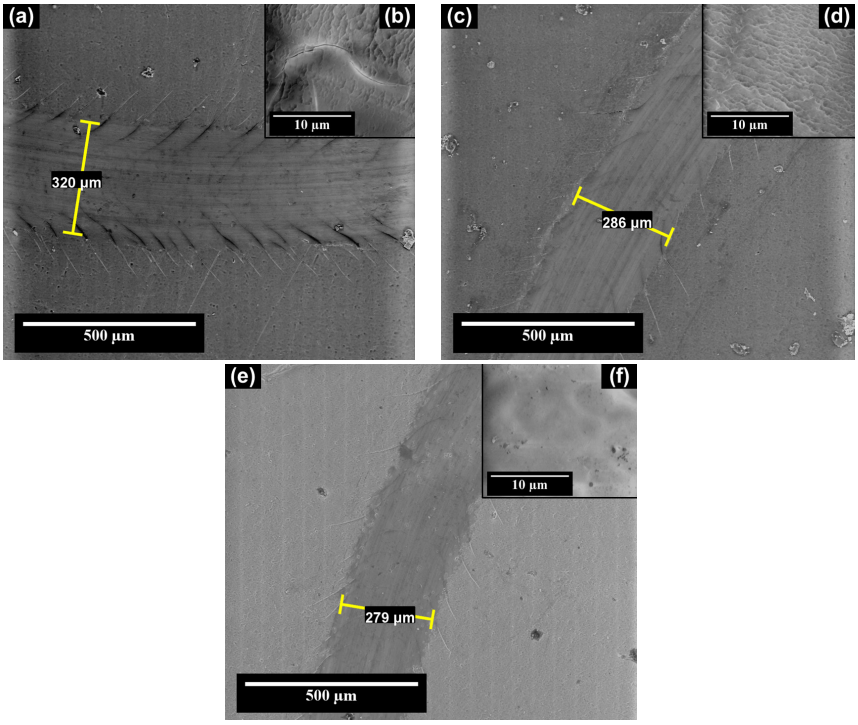


**Figure 5.9.** SEM micrographs of the wear tracks formed on the anodized surfaces for (a) 25 minutes, (c) 35 minutes and (e) 45 minutes at 21 V and 500 rpm electrolyte stirring rate. (b), (d) and (f) SEM micrographs taken inside the wear tracks at an increased resolution

## 5.3. Determination of 2D and 3D profiles of wear tracks

The 2D profiles of the wear tracks formed on the analyzed samples were carried out using Mytutoyo Surftest SJ-210 roughness tester by moving the stylus tip for 2.5 mm with 0.5 µm/s measuring speed.

The 3D profiles were obtained by processing the SEM micrographs of the wear tracks using ImageJ 1.50i software developed by National Institute of Health, USA, (http:\\www.imagej.nih.gov\ij). Using math functions that associate the gray intensity with the heights/roughness of the analyzed surfaces, the software converts the gray intensity in numbers that are exposed on Z axis. A decreased intensity of gray causes the decreasing of values from the Z axis and an increased intensity of gray cause the increasing of Z axis values and so, the 3D profiles of the wear tracks formed on the nanoporous aluminum oxide layers are obtained.

The 2D and 3D profiles reveal that the formed tribolayers in the contact between alumina ball and the nanoporous aluminum oxide layers are compact and uniform in comparison with the tribolayer formed on the electropolished 1050 aluminum alloy. The increasing of the anodic potential and the anodic oxidation process duration cause the formation of more uniform and compact tribolayers on the nanoporous aluminum oxide layers.

From the SEM micrographs and 2D and 3D profiles analysis reveal that the

electropolished 1050 aluminum alloy present an adhesive wear mechanism, the nanoporous aluminum oxide layers obtained at 15 V present a mixt adhesive and abrasive wear mechanism and for the nanoporous aluminum oxide layers anodized at 18 V and 21 V it can be identified an abrasive wear mechanism.

## 5.4. Quantitative characterization of wear tracks

In order to evaluate the tribological properties of the nanoporous aluminum oxide layers obtained by anodic oxidation processes, after the friction assays, the wear volume loss (quantity of loss material during the friction tests) and also the wear rate was calculated.

The wear volume loss ($V_u$) was calculated using the (5.4) eqution [5.15]:

$$V_u = \pi D(\arcsin(\frac{L_u}{2r})r^2 - (L\frac{\sqrt{4r^2 - L_u^2}}{4})) \quad (5.4)$$

where:

D = wear tracks diameters (10 mm);

$L_u$ = wear tracks width (mm);

r = alumina ball radius (10 mm).

The wear rate (k) was calculated using (5.5) equation [5.15]:

$$k = \frac{V_u}{PS} \quad (5.5)$$

where:

Vu = wear volume loss ($mm^3$);

P = normal force (5 N);

S = sliding distance (30 m).

The evolution of the volume loss and wear rate confirm that the nanoporous aluminum oxide layers have an increased wear resistance in comparison with the electropolished 1050 aluminum alloy. The increasing of applied potential, the anodic oxidation process duration and the electrolyte stirring rate cause the nanoporous aluminum oxide layer formation with improved wear behavior.

## 5.5. Partial conclusions

The mechanical properties of the nanoporous aluminum oxide layers anodized in 1 M $H_2SO_4$ in which was added 1 g/L $Al_2(SO_4)_3$ x $18H_2O$, at different electrochemical parameters were evaluated during friction assays using in-situ (friction coefficients) and ex-situ (morphological characterization, 2D and 3D profiles) methods.

The mechanical properties of the nanoporous aluminum oxide layers were compared with the mechanical properties of electropolished 1050 aluminum alloy and also, the influence of electrochemical parameters imposed in the anodic oxidation processes on the wear resistance of the nanoporous aluminum oxide layers formed was evaluated.

Analyzing the friction coefficient diagrams it can be seen that the nanoporous

aluminum oxide layers present decreased value in comparison with the electropolished 1050 aluminum alloy. Also, by increasing the value of imposed potential, the friction coefficients mean values decrease and by increasing the anodic oxidation process duration, the values of the friction coefficients values increase, for both static and dynamic electrolyte regime.

Even if the imposed potential or anodic oxidation process duration are similar, the nanoporous aluminum oxide layers anodized at 500 rpm electrolyte stirring rate present lower values of friction coefficients in comparison with the nanoporous aluminum oxide layers obtained at 0 rpm electrolyte stirring rate.

The SEM micrographs reveal that the wear tracks formed on the nanoporous aluminum oxide layers have decreased width in comparison with the wear track formed on the electropolished 1050 aluminum alloy. The increasing of imposed potential and/or anodic oxidation process duration cause the decreasing of mean values of wear tracks widths. Also, the decreasing of the wear tracks widths is caused by the increasing of the electrolyte stirring rate.

## 5.6. Selective references of chapter 5

[5.1] P.J. Blau, The significance and use of the friction coefficient, Tribology International, 34, (2001), 585 – 591, DOI: 10.1016/S0301-679X(01)00050-0
[5.2] K. Holmberg, A. Matthews, Coatings tribology, properties, mechanisms, techniques and applications in surface engineering 2nd Edition, Elsevier, Amsterdam, Olanda, 2009, ISBN: 978-0-444-52750-9
[5.7] A.R. Riahi, A.T. Alpas, The role of tribo-layers on the sliding wear behavior of graphitic aluminum matrix composites, Wear, 251, (2001) 1396 – 1407, DOI: 10.1016/S0043-1648(01)00796-7
[5.8] W. Bensalah, K. Elleuch, M. Feki, M. Wery, H.F. Ayedi, Mechanical and abrasive wear properties of anodic oxide layers formed on aluminum, Journal of Material Science and Technology, 25, (2009), 508 – 512, ISSN: 1005-0302, http://www.jmst.org/EN/Y2009/V25/I04/508 (accesat în data de 09 ianuarie 2018)
[5.10] N. Tsyntsaru, B. Kavas, J. Sort, M. Urgen, J.-P. Celis, Mechanical and frictional behaviour of nano-porous anodised aluminium, Materials Chemistry and Physics, 148, (2014), 887 – 895, DOI: 10.1016/j.matchemphys.2014.08.066
[5.13] P. Groche, F. Resch, Dry forming of aluminum alloys – Wear mechanisms and influencing factors, Materialwissenschaft und Werkstofftechnik (Materials Science & Engineering Technology), 46, (2015), 813 – 828, ISSN: 1521-4052, DOI: 10.1002/mawe.201500429
[5.15] D. Zhang, G. Dong, Y. Chen, Q. Zeng, Electrophoretic depostion of PTFE particles on porous anodic aluminum oxide film and its tribological properties, Applied Surface Science, 290, (2014), 466 – 474, DOI: 10.1016/j.apsusc.2013.11.114

# CHAPTER 6.

## The correlation between the electrochemical parameters imposed in anodic oxidation process with the wetting, corrosion and wear resistance properties of nanoporous aluminum oxide layers

The development of functional surfaces on different materials change the wetting, anticorrosive and wear resistance properties of support materials. The evaluation of wetting properties influence on anticorrosive and wear resistance properties of materials had drawn the researchers' attention. An improving tendency of materials properties simultaneously with the increasing of wetting properties has been identified.

From anticorrosive performances point of view, the fabrication of functional surfaces with increased hydrophobic performances (contact angle > $90^{o}$) after the immersion into electrolyte has shown a reduced active surface (in contact with corrosive environment) due to the entrapped air into pores of surface irregularities, and chloride ions from electrolyte react after a long immersion time with the substrate, offering an improved materials corrosion resistance.

From tribological point of view, the nanopores or surface irregularities can be used as liquid lubricants reservoirs and during the wear assays without lubricants, the nanoporous surfaces with thick walls show a decreased friction coefficient value due to the slow degradation of nanopores walls and concomitant with the nanopores walls degradation, in the contact area, the nanopores are compressed and the degradation in outer region of contact area is slowed down.

In order to obtain nanoporous aluminum oxide layers that present a cumulation of properties, the experimental results were correlated in order to identify the nanoporous aluminum oxide layer that present concomitant an increased polarization resistance, determinated by fitted EIS diagrams, an increased value of contact angle and a decreased value of friction coefficient and also the electrochemical parameters imposed in the anodic oxidation process during that the aluminum oxide layer it was formed.

The evaluation of nanoporous aluminum oxide layers, individually exposed in chapter 3, 4 and 5, depending the electrochemical parameters varied in the anodic oxidation process, it was observed that the increasing of imposed anodic potential increase the polarization resistance values determined by fitted EIS diagrams and also the decreasing of friction coefficients, indifferent by anodic oxidation process length or electrolyte stirring rate. Also, the contact angles values between the nanoporous aluminum oxide layer surfaces and distilled water drops show an increasing trend for the nanoporous aluminum oxide layers obtained at 25 minutes and 35 minutes and a decreasing trend for the nanoporous aluminum oxide layers

obtained at 45 minutes, concomitant with the increasing of imposed anodic potential or electrolyte stirring rate.

Evaluating the influence of anodic oxidation process duration on nanoporous aluminum oxide layer properties it was observed that the increasing of anodic oxidation process duration causes the increasing of corrosion and wear resistances (the friction coefficient values increase concomitant with the decreasing of wear volume). The nanoporous aluminum oxide layers obtained at 15V and 18 V show an increasing trend of contact angles values simultaneously with the increasing of anodic oxidation process duration in comparison with the decreasing trend of the nanoporous aluminum oxide layers obtained at 21 V.

In table 6.1 the contact angles, the polarization resistances and friction coefficients values obtained are exposed for the nanoporous aluminum oxide layers ranging all imposed parameters during the anodic oxidation processes.

***Table 6.1.*** *The correlation between the electrochemical parameters and the properties of nanoporous aluminum oxide layers*

| **Anodic oxidation parameters** | | | **Contact angle [$^o$]** | **Polarization resistance (EIS) [MΩ]** | **Friction coefficient** |
|---|---|---|---|---|---|
| **Potential [V]** | **Time [min]** | **Stirring rate [rpm]** | | | |
| 15 | 25 | 0 | 80.89 | 0.262 | 0.3729 |
| 15 | 25 | 500 | 82.94 | 0.562 | 0.363 |
| 15 | 35 | 0 | 84.84 | 1.54 | 0.3874 |
| 15 | 35 | 500 | 86.13 | 2.07 | 0.3869 |
| 15 | 45 | 0 | 87.22 | 2.33 | 0.4068 |
| 15 | 45 | 500 | 93.53 | 2.596 | 0.461 |
| 18 | 25 | 0 | 82.09 | 1.172 | 0.2558 |
| 18 | 25 | 500 | 83.94 | 1.201 | 0.238 |
| 18 | 35 | 0 | 85.17 | 3.442 | 0.2729 |
| 18 | 35 | 500 | 87.02 | 3.661 | 0.256 |
| 18 | 45 | 0 | 87.16 | 3.851 | 0.3476 |
| 18 | 45 | 500 | 92.11 | 4.105 | 0.3172 |
| 21 | 25 | 0 | 89.92 | 10.32 | 0.2388 |
| 21 | 25 | 500 | 100.17 | 11.42 | 0.2029 |
| 21 | 35 | 0 | 89.54 | 22.12 | 0.2644 |
| 21 | 35 | 500 | 95.58 | 24.21 | 0.2352 |
| 21 | 45 | 0 | 86.02 | 33.85 | 0.3111 |
| 21 | 45 | 500 | 90.51 | 36.85 | 0.2732 |

The experimental results recorded for the nanoporous aluminum oxide layers obtained at 500 rpm electrolyte stirring rate are exposed in figure 6.2.

By analyzing the values presented in figure 6.2. it can be observed that the increasing of anodic oxidation process duration, the nanoporous aluminum oxide layers anodized at 15 V and 18 V respectively, present an increasing trend of contact angles values simultaneously

with the increasing of polarization resistances obtained by fitted EIS diagrams and with the increasing of friction coefficients.

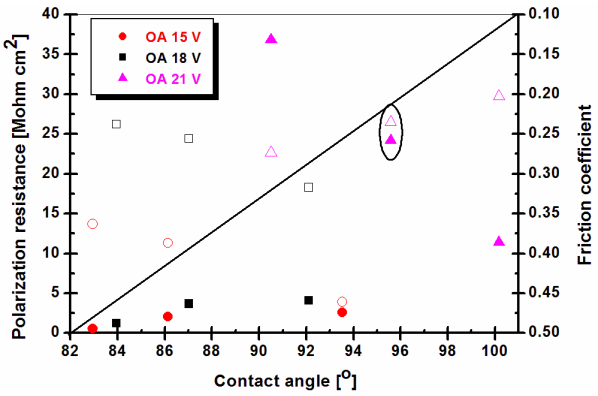


**Figure 6.2.** Representation of polarization resistance (filled symbols) and friction coefficients (empty symbols) depending of contact angles values of nanoporous aluminum oxide layers obtained at an imposed anodic potential between 15 V and 21 V, a duration of anodic oxidation process between 25 minutes and 45 minute and 500 rpm electrolyte stirring rate.

By analyzing the evolution of wetting properties it can be seen an increasing trend of contact angles values for the nanoporous aluminum oxide layers obtained at 25 minutes and 35 minutes, respectively, and a decreasing trend for the nanoporous aluminum oxide layers obtained at 45 minutes simultaneously with the increasing of anodic potential imposed in the anodic oxidation process.

Depending by the anodic oxidation process duration, it can be seen that the nanoporous aluminum oxide layers have increased polarization resistance and friction coefficients concomitant with the increasing of anodic oxidation process duration. The wetting properties show an increasing trend for the nanoporous aluminum oxide layers obtained at 15 V and 18 V and a decreasing trend for the nanoporous aluminum oxide layers anodized at 21 V simultaneously with the increasing of anodic oxidation process duration.

From figure 6.2 it can bee seen that the nanoporous aluminum oxide layers anodized at 15 V and 21 V have decreased values of polarization resistances and increased values of friction coefficients in comparison with the values recorded for the nanoporous aluminum oxide layers obtained at 21 V.

Analyzing the nanoporous aluminum oxide layers anodized at 21 V it can be observed that the layer obtained at 25 minutes has low values of polarization resistance and friction coefficient and also high value of contact angle and the nanoporous aluminum oxide layers anodized at 21 V and 45 minutes has high values of polarization resistance and friction coefficient and a low value of contact angle. The nanoporous aluminum oxide layer obtained at 21 V and 35 minutes has mean values of analyzed properties, being the aluminum oxide layers that show concomitant wear and corrosion resistance and also hydrophobic properties in contact with distilled water droplets.

# CHAPTER 7.

# General conclusions, Perspectives and Future research direction

## 7.1. General conclusions

### 7.1.1. General conclusions on imposed parameters in nanoporous aluminum oxide layers fabrication process on 1050 aluminum alloy

In order to grow nanoporous aluminum oxide layers on 1050 aluminum alloy, the optimum electrolyte, the optimum methods to prepare the aluminum substrate and also, the optimum values of imposed electrochemical parameters in the anodic oxidation process to obtain nanoporous aluminum oxide layers with an uniform cellular structure were identified.

The scientific research aim was to evaluate the influence of imposed electrochemical parameters in the anodic oxidation process on the morphological, structural, composition, roughness and wetting properties of the nanoporous aluminum oxide layers obtained. Also, the optimum values of the electrochemical parameters in order to produce nanoporous aluminum oxide layers with improved corrosion behavior and wear resistance were identified.

By analyzing the cross-section SEM micrographs, the nanoporous aluminum oxide layers thickness could be identified simultaneously with the increasing of the anodic potential and anodic oxidation process duration. The increasing of the electrolyte stirring rate from 0 rpm to 500 rpm lead to the nanoporous aluminum oxide layers thickness decrease, regardless of the applied potential values or anodic oxidation process duration.

The top-view SEM micrographs recorded on the nanoporous aluminum oxide layers surfaces reveal that the increasing of anodic potential and anodic oxidation process duration increases the porosity of aluminum oxide layers obtained, and nanoporous aluminum oxide layers obtained at 500 rpm electrolyte stirring rate, in comparison with the nanoporous aluminum oxide layers obtained at 0 rpm show an increased number of defects.

Analyzing the weight percent of aluminum and oxygen elements from SEM-EDX spectrums it is confirmed that nanoporous aluminum oxide layers are formed on electropolished 1050 aluminum alloy by anodic oxidation process, and presence of sulphur element in SEM-EDX specters confirm that, the electrolyte used in the anodic oxidation process is based on sulphuric acid.

The surfaces of electropolished 1050 aluminum alloy suffered morphological and compositional changes during the anodic oxidation process, regardless of the electrochemical parameter values, due to the formation of the nanoporous aluminum oxide layers.

### 7.1.2. General conclusions on characterization and performances of nanoporous aluminum oxide layers obtained by anodic oxidation on 1050 aluminum oxide

The 2D roughness profiles recorded on the nanoporous aluminum oxide layers reveal that the nanoporous aluminum oxide layers anodized at 15 V and 18 V show a decreasing trend comparing with the 2D roughness profile recorded on electropolished 1050 aluminum alloy. The roughness parameter Ra, calculated from 2D roughness profile recorded on the nanoporous aluminum oxide layer surface anodized at 21 V show an increasing trend simultaneously with the increasing of anodic oxidation process duration for both static or dynamic electrolyte stirring regime.

The mean values of contact angles calculated for the nanoporous aluminum oxide layers show an increasing trend for the anodic potential of 15 V and 18 V and a decreasing trend for the anodic potential of 21 V concomitant with the increasing of anodic oxidation process duration.

The corrosion behavior of the nanoporous aluminum oxide layers were measured after the immersion in 3.5% NaCl solution, using electrochemical corrosion assay and were compared with the corrosion behavior of electropolished 1050 aluminum alloy.

Analyzing the OCP diagrams it was observed that the nanoporous aluminum oxide layers present noble values of free potential steady state in comparison with the electropolished 1050 aluminum alloy free potential steady state. Increasing the values of electrochemical parameters, the recorded free potential steady state shows a decreasing trend.

The EIS diagrams were fitted using equivalent circuits and it was observed that the increasing of anodic potential and anodic oxidation process duration cause the formation of nanoporous aluminum oxide layers with improved corrosion resistance.

Analyzing the potentiodynamic polarization curves it was seen that the passive domains duration increase and the current density values in the passive and transpassive domains decreases simultaneously with the increasing of electrochemical parameters values imposed in anodic oxidation process.

The cyclic voltammograms reveal that the increasing of electrochemical parameters imposed in anodic oxidation process cause the obtaining of nanoporous aluminum oxide layers with a decreased pitting corrosion susceptibility.

The wear resistance of nanoporous aluminum oxide layers was evaluated using friction tests without lubricants.

The friction coefficients diagrams recorded for the nanoporous aluminum oxide layers show that the decreasing trend simultaneously with the increasing of anodic potential value imposed and decreasing of anodic oxidation duration, for both static and dynamic electrolyte stirring regime. Also, it was observed that the increasing of electrolyte stirring rate from 0 rpm to 500 rpm, the obtained nanoporous aluminum oxide layers have decreased friction coefficient values.

The SEM micrographs of the wear tracks formed on nanoporous aluminum oxide layer surfaces reveal a decreasing trend of wear tracks width simultaneously with the increasing value of electrochemical parameters imposed in the anodic oxidation process.

Analyzing the 2D and 3D roughness profiles of wear tracks formed on nanoporous aluminum oxide layers surfaces it is observed the formation of uniform and compact tribolayers concomitant with the increasing of electrochemical parameters values imposed in anodic oxidation process.

Analyzing the SEM micrographs and the 2D and 3D profiles of the wear tracks it was seen that the 1050 aluminum substrate show an adhesive wear mechanism, the nanoporous aluminum oxide layers anodized at 15 present a mixed adhesive and abrasive wear mechanism and the nanoporous aluminum oxide layers formed at 18 V and 21 V show an abrasive wear mechanism.

Also, the wear volume loss and wear rate show a decreasing trend simultaneously with the increasing of the electrochemical parameters imposed in the anodic oxidation process and confirm the improving of wear resistance performance of nanoporous aluminum oxide layers obtained.

## 7.2. Perspectives and Future research direction

- Fabrication of nanoporous aluminum oxide layers by controlled anodic oxidation process on different aluminum alloys.
- Evaluation of $Al_2(SO_4)_3$ x 18 $H_2O$ concentration added into electrolyte on the nanoporous aluminum oxide layers characteristics.
- Optimization of the electrochemical parameters imposed in the anodic oxidation processes in order to obtain nanoporous aluminum oxide layers with ordered structures.
- Evaluation of tribocorrosion performances of the nanoporous aluminum oxide layers.
- Evaluation of corrosion behavior of nanoporous aluminum oxide layers after salt spray exposure.
- Evaluation of corrosion behavior of nanoporous aluminum oxide layers after a long exposure to corrosive environments.
- Determination of organic coatings adhesion to the nanoporous aluminum oxide layer surfaces.
- Evaluation of scratch resistance, determination of nanoporous aluminum oxide layer hardness and Young modulus.
- Evaluation of wear resistance of nanoporous aluminum oxide layers in lubricants presence.

# CHAPTER 8.

# Own contributions and Scientific achievements in the research domain

## 8.1. Own contributions

Elaboration of a bibliographic study based on scientific articles on the developing and characterization methods of the nanoporous aluminum oxide layers using electrochemical methods such as anodic oxidation.

Identification of optimum methods used to prepare the aluminum substrate in order to grow on their surfaces nanoporous aluminum oxide layers using electrochemical methods.

Identification of the electrochemical parameter domain values: potential, duration and electrolyte stirring rate that are imposed in the anodic oxidation processes in order to obtain nanoporous aluminum oxide layers.

Fabrication of nanoporous aluminum oxide layers ranging the electrochemical parameters and the result replication by 20 times in order to observe the processes reproducibility.

Elaboration of the methods used to evaluate the nanoporous aluminum oxide layers properties.

The morphological, structural, compositional, roughness and wetting properties evaluation of the nanoporous aluminum oxide layers obtained by anodic oxidation.

The measuring of nanoporous aluminum oxide layers thickness using cross-section SEM micrographs.

Identification of optimum electrochemical corrosion assays to evaluate the corrosion behavior of the nanoporous aluminum oxide layers.

Evaluation of the corrosion behavior of nanoporous aluminum oxide layers in comparison with the corrosion resistance of the electropolished 1050 aluminum alloy.

Designing and carrying out the complex plane to evaluate the wear behavior of the nanoporous aluminum oxide layers.

The analysis of the obtained experimental data after the characterization of nanoporous aluminum oxide layers, dissemination of obtained results by scientific articles publication and international and national conferences participation.

## 8.2. Scientific achievements in the field of research theme

### 8.2.1. ISI and ISI Proceedings Volume publications

1) Valentin Marian Dumitraşcu, Lidia Benea, **Improving the corrosion behaviour of 6061 aluminum alloy by controlled anodic formed oxide layer**, *Revista de Chimie*, Vol. 68, p.77–80, (2017), ISSN: 2537-5733, http://www.revistadechimie.ro/article_ro.asp?ID=5393 (accessed in 8 January 2018) I.F. 2016 = 1.232

2) Valentin Dumitraşcu, Lidia Benea, Eliza Dănăilă, **Characterization of nanoporous aluminum oxide layers obtained by controlled anodic oxidation**, *Proceedings of 17th International Multidisciplinary Scientific GeoConference SGEM 2017,* Vol. 17 – Micro and Nano Technologies, p. 43–50, 2017, ISSN: 1314-2704.
DOI: 10.5593/sgem2017/61/S24.006

3) Valentin Dumitraşcu, Lidia Benea, Eliza Dănăilă, **Influence of the sealing process on the corrosion performance of nanoporous aluminum oxide**, *Proceedings of 17th International Multidisciplinary Scientific GeoConference SGEM 2017,* Vol. 17 – Micro and Nano Technologies, p. 171–178, 2017, ISSN: 1314-2704.
DOI: 10.5593/sgem2017/61/S24.023

4) Valentin Dumitraşcu, Lidia Benea, Eliza Dănăilă, **Corrosion behaviour of aluminum oxide film growth by controlled anodic oxidation**, *IOP Conference Series: Materials Science and Engineering*, Vol. 209, 2017, Article number 012016, ISSN: 1757-8981.
DOI: 10.1088/1757-899X/209/1/012016

5) Valentin Marian Dumitraşcu, Lidia Benea, Laurenţiu Mardare, **Influence of anodizing voltage on the morphology and corrosion resistance of 1050 aluminum alloy**, *Proceedings of 16th International Multidisciplinary Scientific GeoConference SGEM 2016, Book 6 – Nano, Bio and Green – Technologies for a Sustainable Future*, Vol. 1 – Micro and Nano Technologies, Advances in Biotechnology, p. 167–174, 2016, ISSN: 1314-2704.
DOI: 10.5593/SGEM2016/B61/S24.022

6) Lidia Benea, Valentin Marian Dumitraşcu, **Hybrid composite layers obtained by electro-codeposition: challenges – results and future applications**, *Proceedings of 16th International Multidisciplinary Scientific GeoConference SGEM 2016, Book 6 – Nano, Bio and Green – Technologies for a Sustainable Future*, Vol. 1 – Micro and Nano Technologies, Advances in Biotechnology, p. 151–158, 2016, ISSN: 1314-2704.
DOI: 10.5593/SGEM2016/B61/S24.020

7) Laurenţiu Mardare, Lidia Benea, Valentin Dumitraşcu, **Behavior of naval steel with polymer protective coatings in sea water**, *Proceedings of 16th International Multidisciplinary Scientific GeoConference SGEM 2016, Book 6 – Nano, Bio and Green – Technologies for a Sustainable*

*Future*, Vol. 2 – Green Buildings Technologies and Materials, Green Design and Sustainable Architecture, p. 49–56, 2016, ISSN: 1314-2704.
DOI: 10.5593/SGEM2016/B62/S26.007

8) Doinița Pîrvu-Neagu, Lidia Benea, Valentin Marian Dumitraşcu, Laurențiu Mardare, **Some corrosion problems in municipal waste water collection system of Galati**, *Proceedings of 16th International Multidisciplinary Scientific GeoConference SGEM 2016, Book 5 – Ecology, Economics, Education and Legislation,* Vol. 2 – Ecology and Environmental Protection, p. 743–750, ISSN: 1314-2704.
DOI: 10.5593/SGEM2016/B52/S20.096

9) Lidia Benea, Eliza Dănăilă, Valentin Marian Dumitraşcu, Pierre Ponthiaux, **The effect of anodic oxidation treatment of Ti-10Zr alloy on tribocorrosion behavior in a simulated physiological solution**. *Proceedings of the 5th IEEE International Conference on E-Health and Bioengineering - EHB 2015*, IEEE Xplore Conference Publications. ISBN: 978-1-4673-7545-0.
DOI:10.1109/EHB.2015.7391574

## 8.2.2. Publication in journals indexed in other international research databases

1) Lidia Benea, Eliza Dănăilă, Valentin Marian Dumitraşcu, **Vegetable extracts as inhibitors of carbon steel corrosion in acidic environment**. *Advanced Materials Research*, Vol. 1139, p.46–51, 2016, ISSN: 1662-8985.
DOI: 10.4028/www.scientific.net/AMR.1139.46
The journal Advanced Materials Research, ISSN: 1662-8985, is indexed by:
**Index Copernicus Journals Master List:** www.indexcopernicus.com.
**Google Scholar:** scholar.google.com.
**Chemical Abstracts (CAS)**: www.cas.org.
**Cambridge Scientific Abstracts (CSA):** www.csa.com.
**Inspec (IET, Institution of Engineering Technology):** www.theiet.org.
**SCImago Journal & Country Rank (SJR):** www.scimagojr.com.
**ProQuest:** www.proquest.com.
**EBSCO:** www.ebsco.com.

2) 4. Lidia Benea, Valentin Dumitraşcu, Eliza Dănăilă, Iulian Bounegru, **Electrochemical behavior of cobalt - chromium alloy as biomaterial in different pH environments**. *Advanced Materials Research*, Vol. 1139, p.59–63, 2016, ISSN: 1662-8985.
DOI: 10.4028/www.scientific.net/AMR.1139.59
The journal Advanced Materials Research, ISSN: 1662-8985, is indexed by:
**Index Copernicus Journals Master List:** www.indexcopernicus.com.
**Google Scholar:** scholar.google.com.
**Chemical Abstracts (CAS)**: www.cas.org.
**Cambridge Scientific Abstracts (CSA):** www.csa.com.

**Inspec (IET, Institution of Engineering Technology):** www.theiet.org.
**SCImago Journal & Country Rank (SJR):** www.scimagojr.com.
**ProQuest:** www.proquest.com.
**EBSCO:** www.ebsco.com.

3) Laurenţiu Mardare, Lidia Benea, Eliza Dănăilă, Valentin Dumitraşcu, **Polymeric coatings used against marine corrosion of naval steel EN32**, *Key Engineering Materials*, Vol. 699, p. 71–79, 2016, ISSN: 1662-9795.
DOI: 10.4028/www.scientific.net/KEM.699.71
The journal Key Engineering Materials, ISSN: 1662-9795, is indexed by:
**SCOPUS:** www.scopus.com.
**Index Copernicus Journals Master List:** www.indexcopernicus.com.
**Google Scholar:** scholar.google.com.
**Ei Compendex (CPX):** www.ei.org.
**Chemical Abstracts (CAS):** www.cas.org.
**Cambridge Scientific Abstracts (CSA):** www.csa.com.
**Inspec (IET, Institution of Engineering Technology):** www.theiet.org.
**SCImago Journal & Country Rank (SJR):** www.scimagojr.com.
**ProQuest:** www.proquest.com.
**EBSCO:** www.ebsco.com.
**CiteSeerX:** citeseerx.ist.psu.edu.

4) Georgeta Toderaşcu, Valentin Dumitraşcu, Lidia Benea, Alexandru Chiriac, **Corrosion behaviour and biocompatibility of 316 stainless steel as biomaterial in physiological environment,** *The Annals of "Dunărea de Jos" University of Galaţi, Fascicle IX - Metallurgy and Materials Science*, Vol. 4, p. 16–22, 2015, ISSN 1453-083X.
The journal The Annals of "Dunărea de Jos" University of Galaţi, Fascicle IX - Metallurgy and Materials Science, is indexed by:
**SCIPIO-RO**: http://www.scipio.ro/web/182206
**EBSCO**: http://www.ebscohost.com/titleLists/a9h-journals.pdf,
**Google Academic**: https://scholar.google.ro.

5) Valentin Dumitraşcu, Lidia Benea, **Influence of the anodic oxidation treatment on the corrosion behaviour of aluminium and aluminium alloys**, *The Annals of "Dunărea de Jos" University of Galaţi, Fascicle IX - Metallurgy and Materials Science*, Vol. 3, p. 10–15, 2015, ISSN 1453-083X.
The journal The Annals of "Dunărea de Jos" University of Galaţi, Fascicle IX - Metallurgy and Materials Science, is indexed by:
**SCIPIO-RO**: http://www.scipio.ro/web/182206
**EBSCO**: http://www.ebscohost.com/titleLists/a9h-journals.pdf,
**Google Academic**: https://scholar.google.ro.

6) Adrian Diaconu, Cătălin Solomon, Lidia Benea, Valentin Dumitraşcu, Laurenţiu Mardare, **Corrosion resistance of zinc coated steel in sea water environment**. *The Annals of "Dunărea de Jos" University of Galaţi, Fascicle IX - Metallurgy and Materials Science*, Vol. 3, p. 43–48, 2015, ISSN 1453-083X.
The journal *The Annals of "Dunărea de Jos" University of Galaţi, Fascicle IX - Metallurgy and Materials Science*, is indexed by:
**SCIPIO-RO**: http://www.scipio.ro/web/182206
**EBSCO**: http://www.ebscohost.com/titleLists/a9h-journals.pdf,
**Google Academic**: https://scholar.google.ro.

### 8.2.3. Oral presentation and posters presented at International Scientific Conferences, Workshops and Lectures

1) Valentin Marian Dumitraşcu, Lidia Benea, **Nanostructuration of material surfaces by top-down electrochemical techniques**, *4th Edition of the International Conference "New Trends in Environmental and Materials Engineering" – TEME 2017*, p. 27 – Book of Abstracts, http://www.teme.ugal.ro/Book-of-abstracts.pdf.

2) Lidia Benea, Valentin Dumitraşcu, **Nanostructuration and functionalization of materials and biomaterials by electrochemical methods - a promising route**, *4th Edition of the International Conference "New Trends in Environmental and Materials Engineering" – TEME 2017*, p. 22 – Book of Abstracts,
http://www.teme.ugal.ro/Book-of-abstracts.pdf.

3) Marius Socola, Valentin Marian Dumitraşcu, Sorina Picioruş, Lidia Benea, **Comparative corrosion evaluation of galvanized steel passivated with trivalent and hexavalent chromium solutions**, *4th Edition of the International Conference "New Trends in Environmental and Materials Engineering" – TEME 2017*, p. 21 – Book of Abstracts,
http://www.teme.ugal.ro/Book-of-abstracts.pdf.

4) Valentin Marian Dumitraşcu, Lidia Benea, Eliza Dănăilă, **Characterization of the nanoporous aluminum oxide layer obtained by controlled anodic oxidation**, *17th International Multidisciplinary Scientific GeoConference – SGEM 2017*, Section: Micro and Nano Technologies,
http://www.sgem.org/index.php/sgem-deadline/sgem-programme2017.

5) Valentin Marian Dumitraşcu, Lidia Benea, Eliza Dănăilă, **Influence of the sealing process on the corrosion performance of nanoporous aluminum oxide**, *17th International Multidisciplinary Scientific GeoConference – SGEM 2017*, Section: Micro and Nano Technologies,
http://www.sgem.org/index.php/sgem-deadline/sgem-programme2017.

6) Valentin Marian Dumitraşcu, Lidia Benea, Eliza Dănăilă, Nicoleta Lucica Simionescu,

**Corrosion behavior of aluminum oxide film growth by controlled anodic oxidation**, *International Conference on Innovative Research – ICIR EUROINVENT 2017*, Section I: Synsthesis and characterization of materials, p. 39 – Book of Abstracts, http://www.euroinvent.org/cat/ICIR_2017.pdf.

7) Valentin Marian Dumitrascu, Lidia Benea, **Enhancing the anticorrosion properties of anodic oxide film by sealing process**, *7th Virtual Nanotechnology Poster Conference – Nanoposter 2017*, ID: P17-15, http://www.nanopaprika.eu/group/nanoposter/page/p17-15

8) Valentin Marian Dumitraşcu, Lidia Benea, **Characterization of porous aluminum oxide film obtained by hard anodization**, *11th International Conference on Surface Coatings and Nanostrutured Materials – NANOSMAT 2016*, Section: NanoEngineering, ID: NANO-3, p. 22 – Book of Abstracts, http://www.nanosmat.co.uk/Downloads/Programme%20NANOSMAT%202016%20(FINAL).pdf.

9) Lidia Benea, Valentin Dumitraşcu, **Hybrid composite layers obtained by electro-codeposition: challenges – results and future applications**, *16th International Multidisciplinary Scientific GeoConference – SGEM 2016,* Section: Micro and Nano Technologies, http://www.sgem.org/index.php/sgem-deadline/sgem-programme2016.

10) Valentin Marian Dumitraşcu, Lidia Benea, Laurenţiu Mardare, **Influence of anodizing voltage on the morphology and corrosion resistance of 1050 aluminum alloy**, *16th International Multidisciplinary Scientific GeoConference – SGEM 2016,* Section: Micro and Nano Technologies, http://www.sgem.org/index.php/sgem-deadline/sgem-programme2016.

11) Laurenţiu Mardare, Lidia Benea, Valentin Marian Dumitraşcu, **Behavior of naval steel with polymer protective coatings in sea water**, *16th International Multidisciplinary Scientific GeoConference – SGEM 2016,* Section: Green Buildings Technologies and Materials, http://www.sgem.org/index.php/sgem-deadline/sgem-programme2016.

12) Doiniţa Pîrvu-Neagu, Lidia Benea, Valentin Marian Dumitraşcu, Laurenţiu Mardare, **Some corrosion problems in municipal waste water collection system of Galaţi**, *16th International Multidisciplinary Scientific GeoConference – SGEM 2016,* Section: Ecology and Environmental Protection, http://www.sgem.org/index.php/sgem-deadline/sgem-programme2016.

13) Valentin Marian Dumitrascu, Lidia Benea, **Enhancing corrosion properties of aluminium anodic formed oxide layer by sealing process**, *7th Conference On Material Science & Engineering – UGALMAT 2016*, Section I: Advanced Materials and Technologies (TMA 2016), http://www.ugalmat.ugal.ro/Poster/FINAL%20PROGRAMME%20UgalMat2016.pdf.

14) Lidia Benea, Valentin Marian Dumitraşcu, Pierre Ponthiaux, **Improving the surface properties of Ti-10Zr biomedical alloy by controlled electrochemical oxidation to dorm a thin nanoporous oxide film**, *6th Virtual Nanotechnology Poster Conference – Nanoposter 2016* ID: P16–04,
http://www.nanopaprika.eu/group/nanoposter/page/p16-04.

15) Lidia Benea, Eliza Dănăilă, Valentin Marian Dumitraşcu, Pierre Ponthiaux, **The effect of anodic oxidation treatment of Ti-10Zr alloy on tribocorrosion behavior in a simulated physiological solution,** *The 5th IEEE International Conference on E-Health and Bioengineering – EHB 2015,* Paper ID: 60,
http://www.ehbconference.ro/Portals/0/PROGRAM_DETAILAT.pdf.

16) Laurenţiu Mardare, Valentin Dumitraşcu, Lidia Benea, **Advanced materials and coatings for marine corrosive environment – improving the corrosion resistance of naval steel by polymeric coatings**, *The 3rd International Conference of Young Researchers - New Trends in Environmental and Material Engineering – TEME 2015,*
http://www.teme.ugal.ro.

17) Valentin Dumitraşcu, Lidia Benea, Eliza Dănăilă, **Advanced materials for aerospace applications – influence of anodic oxidation treatment on the corrosion behavior of aluminium and aluminium alloys,** *The 3rd International Conference of Young Researchers - New Trends in Environmental and Material Engineering – TEME 2015*,
http://www.teme.ugal.ro.

18) Laurenţiu Mardare, Lidia Benea, Valentin Dumitraşcu, Eliza Dănăilă, **Polymeric coatings used against marine corrosion of naval steel EN32**, *The 3th International Conference on Polymers Processing in Engineering – PPE 2015*, Symposium 3, Session 2: Polymers, Functional Surface and Interfaces II, PPE2015 – 35,
http://www.if.ugal.ro/PPE2015/PPE2015_Technical_Programe.pdf.

19) Valentin Marian Dumitraşcu, Lidia Benea, Eliza Dănăilă, **Vegetable extracts as inhibitors of carbon steel corrosion in acidic environment**, *International Conference on Sustainable Materials Science and Technology – SMST15*, Session: Materials in research. p. 69 – Book of Abstracts. ISBN: 978-84-944311-0-4,
http://www.scienceknowconferences.com/files/scientific_programs/General_Info_SustainableMaterials.pdf.

20) Lidia Benea, Eliza Dănăilă, Valentin Dumitraşcu, **Influence of electro-codeposition parameters on $TiO_2$ nanoparticles inclusion into nickel matrix: structure, morphology and corrosion resistance,** *15th International Balkan Workshop on Applied Physics – IBWAP 2015*, Session I: Materials Physiscs, S1 O3. p. 29–30 – Book of Abstracts,
http://www.ibwap.ro/2015/uploads/template/BOOK%20of%20Abstracts%20July%202015.pdf.

21) Eliza Dănăilă, Lidia Benea, Valentin Dumitraşcu, Pierre Ponthiaux, **Effects of nano-TiC content on morphology, hardness and tribological properties of Ni/TiC nanocomposite coatings**, *7th EuroNanoForum Conference,* Session: Modelling and characterisation at nanoscale. Poster ID: 1B-113,
http://euronanoforum2015.eu/poster-sessions.

## 8.2.4. Oral presentation and posters presented at National Scientific Conferences, Workshops and Lectures

1) Valentin Marian Dumitraşcu, Lidia Benea, **The influence of the anodizing parameters on the morphology and corrosion resistance of 1050 aluminium alloy**, *5th Edition of Scientific Conference of Doctoral Schools from "Dunărea de Jos" University of Galați*, Section 1: Advanced research in mechanical engineering, industrial engineering and electrical /electronic engineering, O.P. 1.7, p. 36 – Book of Abstracts.
This paper was rewarded with the 2nd prize at Section 1: Advanced research in mechanical engineering, industrial engineering and electrical /electronic engineering.
http://www.cssd-udjg.ugal.ro/index.php/abstracts-2017.

2) Valentin Marian Dumitraşcu, Lidia Benea, Eliza Dănăilă, **Nanoporous alumina film anodic formed on aluminium alloy to enhance the anticorrosion properties in specific environments**, *4th Edition of Scientific Conference of Doctoral Schools from "Dunărea de Jos" University of Galați*, *Session 3: Functional Materials & Nanotechnologies*, O.P. 3.5, p. 45 – 46 – Book of Abstracts.
This paper was rewarded with the 2nd prize at Session 3: Functional Materials & Nanotechnologies.
http://www.cssd-udjg.ugal.ro/files/invitatie/Program_detaliat_al_conferintei_2016.pdf.

3) Valentin Marian Dumitraşcu, Lidia Benea, Eliza Dănăilă, **Electrodeposition of nanocomposite coatings – advantages and challenges**, *3th Edition of Scientific Conference of Doctoral Schools from "Dunărea de Jos" University of Galați, Session 3 & UGALnano 5: Functional Materials & Nanotechnologie*s, O.P. 3.3, p. 81 – Book of Abstracts.
This paper was rewarded with the 3th prize at Session 3 & UGALnano 5: Functional Materials & Nanotechnologies.
http://www.cssd-udjg.ugal.ro/files/invitatie/final/Program_detaliat_al_conferintei_2015_final_corectat.pdf.
http://www.cssd-udjg.ugal.ro/index.php/2015/prizes-2015.